2014

A single-aliquot luminescence dating procedure for K-feldspar based on the dose-dependent MET-pIRIR signal sensitivity

Bo Li
University of Wollongong, bli@uow.edu.au

Richard G. Roberts
University of Wollongong, rgrob@uow.edu.au

Zenobia Jacobs
University of Wollongong, zenobia@uow.edu.au

Sheng-Hua Li
University of Hong Kong, shli@hku.hk

Publication Details

Li, B., Roberts, R. G., Jacobs, Z. & Li, S. (2014). A single-aliquot luminescence dating procedure for K-feldspar based on the dose-dependent MET-pIRIR signal sensitivity. Quaternary Geochronology, 20 51-64.

A single-aliquot luminescence dating procedure for K-feldspar based on the dose-dependent MET-pIRIR signal sensitivity

Abstract
It has been shown previously that the 'sensitivity' of the post-infrared infrared stimulated luminescence (post-IR IRSL or pIRIR) signal—that is, the intensity of the test dose signal (Tx)—can retain a 'memory' of the pre-dose received in nature, but can be reset by sunlight bleaching. Based on this observation, we describe here a single-aliquot regenerative-dose (SAR) multiple elevated temperature (MET) pIRIR dating procedure for K-feldspar that differs in one important respect from the conventional SAR MET-pIRIR procedure. Instead of using a high temperature IR bleaching step between each SAR cycle—as in the conventional procedure—our modified procedure uses a solar simulator bleach for 2 h to reset the dose-dependent pIRIR signal sensitivity before each regenerative SAR cycle. We show that the De can be obtained directly from either the Tx signal or the sensitivity-uncorrected signal (Lx) using the modified procedure. Both of these signals saturate at a higher dose than the sensitivity-corrected signal (Lx/Tx) and, hence, can be used to date older sediments than is feasible using conventional IRSL or pIRIR methods. We have tested our new procedure on 10 sediment samples from different regions of Europe (France and Italy) and Asia (China, Georgia and India), including samples with independently known ages of between ~48 and ~470 ka. Based on these external comparisons of age, and on internal (dose recovery) validation tests of the performance of this new pre-dose MET-pIRIR (or pMET-pIRIR) SAR procedure, we conclude that it can potentially measure natural doses of up to ~1500 Gy in K-feldspar and produce reliable ages for Late and Middle Pleistocene sediments.

Keywords
dependent, met, pirir, signal, sensitivity, luminescence, dating, procedure, k, feldspar, single, dose, aliquot, CAS

Disciplines
Medicine and Health Sciences | Social and Behavioral Sciences

Publication Details
Li, B., Roberts, R. G., Jacobs, Z. & Li, S. (2014). A single-aliquot luminescence dating procedure for K-feldspar based on the dose-dependent MET-pIRIR signal sensitivity. Quaternary Geochronology, 20 51-64.

A single-aliquot luminescence dating procedure for K-feldspar based on the dose-dependent MET-pIRIR signal sensitivity

Bo Li[1,*], Richard G. Roberts[1], Zenobia Jacobs[1], Sheng-Hua Li [2]

[1] Centre for Archaeological Science, School of Earth and Environmental Sciences, University of Wollongong, Wollongong, NSW 2522, Australia

[2] Department of Earth Sciences, The University of Hong Kong, Pokfulam Road, Hong Kong, China

*Corresponding author: bli@uow.edu.au

Abstract

It has been shown previously that the 'sensitivity' of the post-infrared infrared stimulated luminescence (post-IR IRSL or pIRIR) signal—that is, the intensity of the test dose signal (T_x)—can retain a 'memory' of the pre-dose received in nature, but can be reset by sunlight bleaching. Based on this observation, we describe here a single-aliquot regenerative-dose (SAR) multiple elevated temperature (MET) pIRIR dating procedure for K-feldspar that differs in one important respect from the conventional SAR MET-pIRIR procedure. Instead of using a high temperature IR bleaching step between each SAR cycle—as in the conventional procedure—our modified procedure uses a solar simulator bleach for 2 hr to reset the dose-dependent pIRIR signal sensitivity before each regenerative SAR cycle. We show that the D_e can be obtained directly from either the T_x signal or the sensitivity-uncorrected signal (L_x) using the modified procedure. Both of these signals saturate at a higher dose than the sensitivity-corrected signal (L_x/T_x) and, hence, can be used to date older sediments than is feasible using conventional IRSL or pIRIR methods. We have tested our new procedure on 10 sediment samples from different regions of Europe (France and Italy) and Asia (China, Georgia and India), including samples with independently known ages of between ~48 and ~470 ka. Based on

these external comparisons of age, and on internal (dose recovery) validation tests of the performance of this new pre-dose MET-pIRIR (or pMET-pIRIR) SAR procedure, we conclude that it can potentially measure natural doses of up to ~1500 Gy in K-feldspar and produce reliable ages for Late and Middle Pleistocene sediments.

Keywords: K-feldspar, infrared stimulated luminescence, post-IR IRSL, pre-dose, pMET-pIRIR.

1. Introduction

Luminescence dating can determine the burial time of commonly occurring natural minerals such as quartz and feldspar. Optically stimulated luminescence (OSL) dating of quartz has been widely used in the last decade, but the OSL signal usually saturates at relatively low doses (typically less than 300 Gy). This restricts OSL dating of quartz to sediments deposited within the last 200 ka or so, unless the environmental dose rate is exceptionally low. By contrast, the infrared stimulated luminescence (IRSL) signal from K-feldspar (Hütt et al., 1988) saturates at much higher doses than does quartz OSL, so there are advantages in developing a dating method based on IRSL measurements of feldspar. Unfortunately, feldspars have long been known to exhibit 'anomalous' (athermal) fading of the trapped charges related to the IRSL signals (Spooner, 1994; Huntley and Lamothe, 2001; Huntley and Lian, 2006), which results in substantial age underestimates unless appropriate corrections for fading are applied.

Many attempts have been made to correct for, or minimise, the unwanted effect of anomalous fading in IRSL dating (e.g. Sanderson and Clark, 1994; Lamothe and Auclair, 1999; Huntley and Lamothe, 2001; Zhao and Li, 2002; Lamothe et al., 2003; Tsukamoto et al., 2006; Kars et al., 2008; Li et al., 2008). As these methods are model and/or dose dependent (Huntley and Lian, 2006; Li and Li, 2008), it is desirable to make use of an IRSL signal that is not affected by anomalous fading. Recent

progress in understanding anomalous fading in feldspar has raised the prospect of isolating a non-fading IRSL component. This avoids the need to correct for fading based on fading rates measured over laboratory timescales and using models that are valid only at low doses, in the linear portion of the IRSL dose response curve (Huntley and Lamothe, 2001).

Wintle (1973) reported anomalous fading of thermoluminescence (TL) in feldspars, but Valladas and Valladas (1978) and subsequent studies (e.g. Guérin, 2006) found that the high temperature TL of plagioclase feldspars is not affected by fading. Jain and Singhvi (2001) observed that IR bleaching of feldspars at 220 °C resulted in a remnant population of more thermally stable traps that could potentially be probed by high temperature IR stimulation. Following this suggestion, Thomsen et al. (2008) found that IR signals stimulated at 225 °C faded much less than those stimulated at 50 °C, prompting them to propose a post-IR IRSL (pIRIR) procedure for K-feldspar. In their procedure, feldspar grains were first bleached using IR photons at 50 °C and then stimulated again using IR photons while holding the sample at an elevated temperature of 225 °C, to preferentially probe traps that suffer least from fading (Buylaert et al., 2009). This method has since been modified, either by increasing the pIRIR stimulation temperature to 290 °C (Thiel et al., 2011; Buylaert et al., 2012) or by using a multiple elevated temperature (MET) stimulation procedure—the so-called MET-pIRIR procedure (Li and Li, 2011; Li and Li, 2012)—in which the feldspar grains are stimulated with IR at successively higher temperatures, from 50 °C to 300 °C.

In the pIRIR and MET-pIRIR procedures, the basic structure of the single-aliquot regenerative-dose (SAR) procedure (Murray and Roberts, 1998; Galbraith et al., 1999; Murray and Wintle, 2000) is adopted to overcome sensitivity changes induced by different laboratory treatments, which include irradiation, preheating and stimulation. That is, the sensitivity of the regenerative dose signal (L_x) is monitored and corrected for by the corresponding test dose signal (T_x), and the equivalent dose (D_e) is determined from the sensitivity-corrected L_x/T_x and natural (L_n/T_n) signals. The characteristic saturation dose (D_0) of the sensitivity-corrected pIRIR signals is usually less than

~500 Gy, which places an upper bound on D_e estimation of ~1000 Gy if a D_e equal to $2D_0$ is considered a conservative upper limit (Wintle and Murray, 2006; but see Galbraith and Roberts, 2012). This $2D_0$ criterion was originally suggested for quartz OSL, and Li and Li (2012) reported that it is possible to reliably measure D_e values larger than $2D_0$ using K-feldspar from Chinese loess samples.

Recently, a strong pre-dose dependence in the sensitivity of the MET-pIRIR signal, manifested by the response of the T_x signal, has been reported by Li et al. (2013b). We found that the sensitivity of the MET-pIRIR T_x signal increases with the pre-dose received in the preceding regenerative cycles and, furthermore, that it saturates at a much higher dose (D_0 ~750 Gy) than the sensitivity-corrected signal (L_x/T_x) (D_0 ~400 Gy). Based on the observation that the sensitivity of the MET-pIRIR T_x signal can be depleted by sunlight bleaching or by heating, Li et al. (2013b) proposed a multiple-aliquot regenerative-dose (MAR) MET-pIRIR dating procedure, which allows dating of K-feldspar using the dose-dependent sensitivity in T_x. This procedure was tested on aeolian sediments from northern China that have ages ranging from modern to 470 ka. We found that this method can measure D_e values of up to ~1500 Gy and produce ages consistent with the expected ages for the samples investigated. In the present study, we examine the effects of simulated sunlight bleaching and preheating treatment on the signals and develop a single-aliquot dating procedure based on their dose-dependent sensitivity changes. We apply this method to a range of samples from different regions, several of which have independent age control, and show that this new pre-dose MET-pIRIR (pMET-pIRIR) technique can cover a much broader time range than can currently be dated using K-feldspar or quartz.

2. Sample descriptions

Ten sediment samples were examined in this study to assess the variability in the properties of K-feldspars from different regions of Eurasia. The sample locations, expected D_e values and expected depositional ages are summarized in Table 1. The samples were deposited in a variety of

environmental settings between ~48 and ~470 ka ago, and have natural doses ranging from ~100 to ~1600 Gy. The loess samples (LC-110, LC-230 and LC-270) were taken from the Luochuan section at the Chinese Loess Plateau (CLP), and these have been used previously for testing the MET-pIRIR method (Li and Li, 2012). The aeolian sand samples (Sm1, Sm5, Sm6' and Sm8) were collected from the Shimao section (Sun et al., 1999) at the southeastern margin of the Mu Us Desert (MUD) in central China; these samples were used to investigate the dose-dependent sensitivity changes in our previous study (Li et al., 2013b). Two samples (DHB2-OSL4 and PIN-OSL2) consist of colluvial and alluvial sediments deposited at open-air archaeological sites in north-central India and in the southern Caucasus, Georgia, respectively. The two remaining samples were collected from a colluvial–alluvial palaeosol sequence in Italy (CEP-OSL1) and from a collapsed cave in France (LC10-16).

Independent age controls of these samples extend from ~48 to ~470 ka (Table 1), providing an order-of-magnitude time range to test our new method. The chronology of the Luochuan and Shimao sections has been established previously based on stratigraphic correlation (Sun et al., 1999; Ding et al., 2002). Sample LC10-16 has a single-grain quartz OSL age of 47.9 ± 3.3 ka (Jacobs et al., unpublished data) and radiocarbon ages of 42.4–43.8 cal. ka BP have been obtained from bones recovered from the overlying and underlying archaeological layers (Talamo et al., 2012). There are no firm independent age controls for samples DHB2-OSL4, PIN-OSL2 and CEP-OSL1, but the latter pair is expected to date to the Middle Pleistocene and DHB2-OSL4 to the Late Pleistocene, based on their archaeological and geological contexts. These three samples were selected for purposes of studying their luminescence behaviours.

3. Experimental procedures and analytical facilities

The samples were prepared for IRSL analysis using routine procedures (Aitken, 1998). First, the samples were treated with HCl acid and H_2O_2 solution to remove carbonates and organic matter, respectively, and then dried and sieved to obtain grains of 63–90, 90–125, 125–180, 150–180 and 180–212 μm in diameter (Table 1). The K-feldspar grains were separated from quartz and heavy

minerals using a solution of sodium polytungstate with a density of 2.58 g/cm^3. The separated K-feldspar grains were immersed in 10% HF acid for 40 min to etch the surfaces of the grains and remove the outer, alpha-irradiated portions, and then rinsed in HCl acid to remove any precipitated fluorides. After drying, the etched K-feldspar grains were mounted as a monolayer on stainless steel discs of 9.8 mm diameter using "Silkospray" silicone oil as an adhesive. Grains covered the central ~5 mm diameter portion of each disc, corresponding to several hundreds to thousands of grains per aliquot.

IRSL measurements were made on an automated Risø TL-DA-20 reader equipped with IR diodes for stimulation (870 Δ 40 nm). The total IR power delivered to the sample position was ~135 mW/cm^2 (Bøtter-Jensen et al., 2000) and laboratory irradiations were carried out on the reader using a calibrated ^{90}Sr/^{90}Y beta source. IRSL signals were detected by an Electron Tubes Ltd 9235B photomultiplier tube fitted with Schott BG-39 and Corning 7-59 filters to restrict transmission to 320–480 nm. Each IRSL measurement was made for 100 s (Table 2), and the resulting signal was calculated as the sum of counts over the initial 10 s of stimulation, with 'late light' subtraction (Aitken, 1998) of the background count rate over the final 10 s of stimulation. We note that the IRSL intensity does not reach a constant level after 100 s of stimulation, but continues to decay; so the subtracted background consists of 'dark' counts intrinsic to the photomultiplier tube, scattered incident photons, and IRSL associated with the eviction of electrons from traps that are sensitive to IR photons at the chosen stimulation temperature. For each IRSL measurement, an 'IR-off' period was applied to monitor and minimise the isothermal decay signal (Fu et al., 2012); that is, the aliquots were held for 10, 10, 20, 20 and 50 s at the stimulation temperatures of 50, 100, 150, 200 and 250 °C, respectively, before switching on the IR diodes to induce the IRSL signal.

4. The multiple-aliquot pre-dose MET-pIRIR procedure

In our previous study (Li et al., 2013b), we proposed a multiple-aliquot regenerative-dose (MAR) procedure for determining ages using the dose-dependent sensitivities of the feldspar IRSL

signals as a practical method to extend the dating range of feldspars. In this MAR method, the samples were divided into several groups of aliquots, each consisting of 4–6 aliquots. One group was used to measure the natural signals, and the other groups were bleached using a Dr Hönle solar simulator (model: UVACUBE 400) for 2 hr and then given different regenerative doses. We showed that a 2 hr bleach by the solar simulator was sufficient to reset the MET-pIRIR signals and their sensitivities to a stable level (Li et al., 2013b). These aliquots were then measured using the MAR procedure shown in Table 2a. This is the same as the standard MET-pIRIR procedure (Li and Li, 2011) for steps 1–14, except that the preheat of 300 °C was held for 60 s in this study in order to avoid isothermal TL signal at 250 °C (following Fu et al., 2012), compared to 10 s by Li and Li (2011). Here we refer to the test dose signals measured in steps 10–14 as T1, rather than T_x, and the test dose signals in steps 16–22 as T2. The T2 signals are important because the 600 °C heating in step 15 erases the pre-dose memory and sensitivity information (Li et al., 2013b). Thus, T2 is independent of the pre-dose received, so these signals were used to normalise for inter-aliquot variations, which is a key requirement for precise D_e determination using any multiple-aliquot procedure. MAR dose response curves (DRCs) were constructed for the standard sensitivity-corrected MET-pIRIR signals (L_x/T1), as well as the normalised test dose signals (T1/T2) and normalised regenerative dose signals (L_x/T2). D_e values were obtained by projecting natural signal (L_n/$T1_n$, L_n/T2 and $T1_n$/T2) onto each of these DRCs. Li et al. (2013b) found that all three yielded consistent D_e values for their samples, but that T1/T2 and L_x/T2 saturate at much higher doses and, hence, can be used to date older samples.

The sensitivity change—that is, the change in T1—may relate to two factors. The first is changes in electron trapping probability from one test dose cycle to another, due to competition among different kinds of traps. The second is changes in recombination probability during IRSL stimulation, which is controlled primarily by the number of holes at luminescence centres and their abundance relative to non-radiative ('killer') centres. Li et al. (2013b) suggested that the dose-dependent change in sensitivity of the pIRIR signal from K-feldspar is due mainly to changes in the recombination probability during IRSL measurements, caused by changes in the number of holes

174 trapped at luminescence centres. They provided two arguments to support this conclusion: 1) changes
175 in trapping probability during irradiation are unlikely to induce a significant dose dependence in
176 sensitivity, whereas Li et al. (2013b), for example, observed a change of almost 300% in the
177 sensitivity of the 250 ºC MET-pIRIR signal from 0 to ~2000 Gy; 2) the low-temperature IRSL and
178 high-temperature MET-pIRIR signals differ significantly in their dose-dependent changes in
179 sensitivity: this cannot be explained by changes in electron trapping probabilities during irradiation,
180 because trapping competition during irradiation should have a similar effect on all traps giving rise to
181 the IRSL and MET-pIRIR signals. Based on these explanations, they assumed that the intensity of L_x
182 is proportional to both the populations of electron trap and hole centres induced by the regenerative
183 dose, and the sensitivity (T1) is proportional only to the population of hole centres. Hence, the
184 sensitivity-corrected signal (L_x/T1) represents the population of electron traps. From the observation
185 that sensitivity (T1) saturates at higher doses than L_x/T1, Li et al. (2013b) concluded that the hole
186 centres (represented by T1) associated with the MET-pIRIR signals have a higher saturation dose
187 level than do the electron traps. Since L_x is proportional to both the populations of the electron traps
188 and the hole centres, it also features a high saturation dose level. We note that, based on IRSL
189 measurements only, one cannot distinguish if the sensitivity change is caused by the relative
190 abundance of luminescence centres compared to "killer" centres, or by an absolute increase in the
191 number of luminescence centres. The latter provides a more straightforward explanation of the dose
192 dependency observed, so we have adopted this mechanism to explain our results. We acknowledge,
193 however, that other possibilities cannot be ruled out, and that more studies are required to reveal the
194 true physical mechanism of this dose dependency.

195 This MAR procedure was tested on aeolian sediments from the Shimao section in northern
196 China that have ages ranging from modern to 470 ka (Li et al., 2013b). It was found that this method
197 produces ages consistent with the expected ages for the samples investigated, suggesting that the
198 MAR method is suitable for old samples with homogeneous behaviours among aliquots. However, the
199 IRSL and pIRIR sensitivities of K-feldspar grains are not only dependent on the natural dose received

since their last exposure to sunlight, but are also on their thermal and pre-dose history (Li et al., 2013b). For example, the sensitivities of the MET-pIRIR signals can be depleted by over 90% by heating to a high temperature, such as ~500–600 °C. Samples may consist, therefore, of grains that were heated to a high temperature by a bushfire or volcanic event before transportation to their final burial place, and other grains that were not heated. As a result, different grains may contain different pre-dose information, giving rise to grain-to-grain variation in pIRIR sensitivity and, hence, differences among aliquots. In such cases, the multiple-aliquot method may not be appropriate.

In this study, we have tested the MAR method (Table 2a) using the sample CEP-OSL1, which provides an example where MAR method is not applicable. It was found that, despite several hundred grains being measured simultaneously on each aliquot, a large variation in T1/T2 ratios was obtained for different aliquots that had been given the same laboratory dose (Fig. 1a) and then measured using the MAR method. This result indicates that different grains may have experienced significantly different dosing and thermal histories before burial, and that hundreds of grains on each aliquot are not necessarily sufficient to average such variation. This is presumably due to the fact that only a small fraction of K-feldspar grains gives rise to a large proportion of the total IRSL signals (Li et al., 2011). We note that the inter-aliquot variation was significantly reduced in the sensitivity-corrected signal L_x/T1 (Fig. 1b), which suggests that the variation observed in Fig. 1a is due mainly to between-aliquot differences in sensitivity. A single-aliquot procedure is required for such samples.

5. The single-aliquot pre-dose MET-pIRIR (pMET-pIRIR) procedure

To overcome the problems of the MAR method associated with inter-aliquot variations, we have developed a single-aliquot procedure that utilises the dose-dependent sensitivities of the K-feldspar IRSL signals (Table 2b). This single-aliquot pMET-pIRIR procedure is similar to the standard MET-pIRIR procedure of Li and Li (2011) except that a 2 hr solar simulator bleaching is given in step 15, rather than a high-temperature IR bleach. The purpose of the solar bleaching is to reset the pre-dose ‘memory’ expressed in the sensitivity of the MET-pIRIR signals, based on the

observation by Li et al. (2013b) that the sensitivity of these signals can be reduced to a stable level after a 2 hr bleach using a UVACUBE 400 solar simulator. If a solar bleach can effectively reset the dose-dependent sensitivity between successive SAR cycles, then T_x should be proportional to L_x and both signals should be a function of regenerative dose given in the preceding step (step 1 in Table 2b), and, hence, can be used for determining D_e values. This protocol is tested in the following sections.

5.1. Sensitivity changes

A key assumption of the single-aliquot procedure in Table 2b is that a 2 hr bleach using a solar simulator can reset the sensitivity of the MET-pIRIR signals to the same level at the end of each SAR cycle, so any pre-dose effect does not carry over from cycle to cycle. A simple test of this assumption is to repeatedly apply the same regenerative dose to an aliquot, measure the resulting pIRIR signals, and examine if there are significant changes in the intensities of the L_x signal. Four groups of 3 aliquots of sample Sm8 were first exposed to the solar simulator for 2 hr. These aliquots were then given a regenerative dose of 1100 Gy and measured using the SAR procedure shown in Table 2b, but using different preheat temperatures of 300, 320, 340 and 360 °C for 60 s at steps 2 and 9 to investigate the effect of thermal treatment on sensitivity change. For each aliquot, the SAR cycle was repeated 6 times using the same regenerative dose and test dose (D_t = 33 Gy). Fig. 2a, b and c show the results for L_x/T_x, L_x and T_x MET-pIRIR (250 °C) signals, respectively, plotted against cycle number for each of the preheats tested. The L_x/T_x values changed negligibly from cycle to cycle for all preheat temperatures (Fig. 2a), indicating that sensitivity changes in L_x are successfully monitored by T_x and, thus, sensitivity correction using T_x is reliable at all preheat temperatures.

This pattern, however, is not true for the L_x and T_x signals themselves (Fig. 2b and 2c). The intensities of L_x and T_x increased by ~15% from cycle 1 to cycle 6 when a preheat of 360 °C was applied. A much smaller increase in intensities was observed for a preheat of 340 °C, and a negligible change in L_x or T_x resulted from preheats of 320 and 300 °C. For the latter pair of preheats, the change in sensitivity varied by less than 5% from the first cycle to the last for both L_x and T_x. The results of

Fig. 2b and c suggest, therefore, that a solar simulator bleach of 2 hr can effectively reset the signal sensitivity between successive SAR cycles for sample Sm8, but only when a preheat of between 300 and 320 °C is applied. In the following studies, we adopted a preheat of 300 °C for all of the samples investigated, and show below that that a 2 hr bleach is sufficiently to reset the sensitivities of their L_x and T_x MET-pIRIR signals.

Fig. 2a, b and c also show the corresponding data (as open circles) obtained using the standard MET-pIRIR procedure of Li et al. (2011), which employs a 'hot' IR bleach for 100 s at 300 °C (instead of a 2 hr solar simulator bleach) at the end of each SAR cycle, and a preheat of 300 °C for 60 s. The changes in the L_x/T_x ratio vary by less than 5% from the first cycle to the last cycle (Fig. 2a), indicating that the sensitivity correction is successful. Larger variations in the intensity of the L_x and T_x signals (Fig. 2b and c) were observed, however, using the standard SAR procedure with a hot IR bleach, when compared to those obtained using a 2 hr solar simulator bleach. For example, the intensity of T_x signal increased by ~10 % from the first cycle to the last (Fig. 2c). This further suggests that a 2 hr solar simulator bleach at the end of each SAR cycle is sufficient to stabilize the sensitivities of the MET-pIRIR signals.

The results in Fig. 2c demonstrate that a solar simulator bleach can reset the sensitivity (or T_x) to a stable level among different SAR cycles when the same regenerative dose (or pre-dose) is applied, but they do not show whether or not this level is dependent on the size of the pre-dose received. To test the latter, we measured the sensitivity (T_x) after a 2 hr solar simulator bleach of 3 samples spanning a 43-fold range of natural doses: Sm1 (37 ± 4 Gy), Sm5 (508 ± 41 Gy) and Sm8 (1593 ± 114 Gy) (Li et al., 2013b). The sensitivity (T_x) of the MET-pIRIR 250 °C signal after bleaching is plotted against the natural dose in Fig. 2d, which shows that T_x reaches a constant level after solar bleaching, even though the natural doses of these samples differ substantially. This result confirms that T_x starts from a constant level that is independent of the size of the pre-dose received.

5.2. Dose response curves

Dose response curves were constructed to test the dose dependency of L_x, T_x and L_x/T_x for samples from different geographic regions. Four aliquots of each sample were measured using the SAR procedure in Table 2b, using a series of regenerative doses including a repeat dose and a zero dose to induce the L_x signals. The test dose signals (T_x) were also measured to track the dose-dependent sensitivities and determine the sensitivity-corrected MET-pIRIR L_x/T_x ratios.

Fig. 3 shows the DRCs for the MET-pIRIR signals measured at different stimulation temperatures from a single aliquot of sample CEP-OSL1; these DRCs are typical of those obtained for other aliquots of this sample and other samples. In Fig. 3a, the sensitivity-corrected 50 °C IRSL and pIRIR signals show different shapes in their DRCs. The 50 °C IRSL signal has the highest sensitivity-corrected intensity. The DRCs for the MET-pIRIR signals at 100 and 150 °C are similar to each other, whereas those for the 200 and 250 °C signals—the latter in particular—saturate at lower L_x/T_x intensities. Each of the DRCs in Fig. 3a can be fitted using a single saturating exponential function (solid lines), and their characteristic saturation dose (D_0) values for the different signals are shown next to each curve. The D_0 value is highest for the IRSL signal measured at 50 °C (~600 Gy) and gradually decreases with increasing stimulation temperature (from ~560 Gy at 100 °C to ~400 Gy at 250 °C). The characteristics of the DRCs shown in Fig. 3a are consistent with the previous observations of Li and Li (2011), and suggest that an upper dose limit of ~800-1000 Gy can be measured for sample CEP-OSL1 using the sensitivity-corrected signals (L_x/T_x).

Compared to L_x/T_x, the normalised intensities of the sensitivity-uncorrected signals (L_x) are far more reproducible at the different stimulation temperatures (Fig. 3b). A common characteristic saturation dose of ~850 Gy was obtained for all DRCs, which suggests that L_x signal could be used to measure a much higher dose (at least 1700 Gy) than can be achieved using L_x/T_x signal, thereby significantly extending the dating limit. The sensitivity of the different MET-pIRIR signals shows a strong dose dependence (Fig. 3c), as indicated by the intensities of the test dose (T_x) signals. The dose dependence is greater for the pIRIR signals measured at higher stimulation temperatures: for example, the MET-pIRIR T_x signal measured at 250 °C increased nearly 4-fold over a dose range of 0–3300

301 Gy, whereas the T_x intensity of the 50 °C IRSL signal increased by only ~70%. The D_0 values for the
302 saturating exponential DRCs fitted to the T_x data are 828 ± 17, 698 ± 50, 677 ± 36, 723 ± 47 and 750
303 ± 40 Gy for the 50, 100, 150, 200 and 250 °C signals, respectively (Fig. 3c). These values are broadly
304 consistent at 2σ and are greater than the D_0 values obtained from the L_x/T_x signals at each of these
305 stimulation temperatures. As L_x/T_x is proportional to the population of electron traps, and as the
306 sensitivity (manifested by the intensity of the T_x signal) represents the population of hole centres, the
307 higher saturation dose level of T_x, relative to L_x/T_x, indicates that the hole centres associated with the
308 IRSL and MET-pIRIR signals saturate at a higher dose than do the electron traps. The single-aliquot
309 results for L_x and T_x are consistent with the L_x/T2 and T1/T2 results obtained using the multiple-
310 aliquot protocol (Li et al., 2013b).

311 Although sunlight can deplete the sensitivity of MET-pIRIR signals, it cannot fully reset them
312 (see Fig. 7b in Li et al., 2013b). This indicates that there are two components of hole centres
313 associated with the MET-pIRIR signals, of which one is bleachable and the other is not. The validity
314 of the DRCs for T_x therefore relies on the assumption that the sensitivity of the bleachable hole
315 centres is fully reset at the end of each SAR measurement cycle, so that T_x does not retain any
316 memory of the doses received in the previous SAR cycles. A test of this assumption is to investigate
317 the relationship between L_x and T_x. Since L_x can be fully reset by the MET-pIRIR measurement in
318 each SAR cycle, it should be linearly correlated to T_x if the pre-dose information contained in T_x is
319 fully erased by solar bleaching and does not accumulate with successive SAR cycles. The values of L_x
320 and T_x shown in Fig. 3b and 3c (for sample CEP-OSL1) are plotted against each other in Fig. 4a. A
321 linear relationship is observed between L_x and T_x at the different MET-pIRIR stimulation
322 temperatures, confirming that T_x is proportional only to the corresponding regenerative dose received
323 in the same SAR cycle, and that any pre-dose memory (of doses given in preceding SAR cycles) has
324 been removed by the 2 hr solar bleach.

We note that, unlike the relationship between L_x and T_x commonly used for OSL dating of quartz, in which the size of the regenerative dose is kept constant (Wintle and Murray, 2006), the data in Fig. 4 were obtained from the results of different regenerative doses, including a zero regenerative dose, for which the T_x values are not zero but the L_x values (the left-most data points next to the y-axis of Fig. 4a) are close to zero. As a result, the relationship between L_x and T_x does not pass through the origin. If these data are normalised to a T_x value of unity at zero dose, it can be seen that the slope of the relationship between L_x and T_x increases with IR stimulation temperature (Fig. 4b). It is interesting to note also that the natural points, L_n and T_n, shown as open symbols in Fig. 4a and b, lie almost exactly on the lines of the best fit to the L_x and T_x signals, indicating that these aliquots of sample CEP-OSl1 were fully bleached by sunlight in antiquity, such that any pre-dose information on sensitivity was reset at the time of sediment deposition.

We have also investigated whether a hot IR bleach can offer a more practical alternative to the solar bleach in terms of resetting the sensitivity from cycle to cycle. One aliquot of sample CEP-OSL1 was measured using the MET-pIRIR procedure with a hot IR bleach for 100 s at 320 °C applied after each SAR cycle. The DRCs for the 250 °C MET-pIRIR L_x/T_x, L_x and T_x signals are shown in Fig. 5a, b and c, respectively. L_x/T_x and L_x yield DRCs that grow monotonically with regenerative dose (Fig. 5a and b) and have recycling and reproducibility ratios of 1.10 ± 0.06 and 0.90 ± 0.04 for L_x/T_x and L_x, respectively. By contrast, the T_x signal has an incoherent DRC, with large scatter observed among the different regenerative doses, and very poor reproducibility (0.80 ± 0.03) of the duplicate regenerative doses at ~440 Gy (Fig. 5c). This result differs from that obtained using a solar simulator bleach after each SAR cycle (Fig. 3c), which is not surprising because the high-energy (e.g. UV) components of the solar spectrum can evict charges from many traps that are not reachable by IR photons, even at elevated temperatures. A further advantage of using a solar simulator bleach is that the sediments were exposed to sunlight and not only IR radiation before burial, so the laboratory solar bleach can reset the sensitivity (T_x) to the same level as that achieved in nature. We conclude,

therefore, that a hot IR bleach at 320 °C does not have the same effect as a solar bleach and that the latter is preferable for resetting T_x, at least for this sample.

Another test of the validity of using a 2 hr solar simulator bleach to erase the pre-dose memory of T_x is to apply a repeat dose during the construction of the DRC, as is usually included in a SAR procedure, and then calculate the ratio for the results obtained from the duplicate doses as a check on reproducibility. A ratio that is equal or close to unity indicates that the pre-dose information does not accumulate with successive cycles and, therefore, the solar bleaching step at the end of each SAR cycle is sufficient to reset the optically bleachable sensitivity. This 'recycling ratio' test is investigated in the next section.

In view of the high D_0 values of the MET-pIRIR T_x signals (Fig. 3c) and the increased intensity of T_x at elevated temperatures (Fig. 4) we applied the SAR procedure in Table 2b to different samples from Eurasia (Table 1). Fig. 6 shows the normalised DRCs of the 250 °C MET-pIRIR signals obtained from these samples. It is interesting that all of the samples have similar normalised DRCs for L_x/T_x, L_x and T_x, despite originating from significantly different geological provinces. Such homogeneous behaviour in the pIRIR properties of K-feldspars from disparate geographic regions suggests that it may be feasible to establish a common or standardised DRC (Roberts and Duller, 2004) for feldspar. Studies using more samples from additional regions are required to confirm the generality of our finding. If a single DRC is fitted to these data using a saturating exponential function (dotted lines in Fig. 6), characteristic saturation doses of ~331, 740 and 637 Gy are obtained for the L_x/T_x, L_x and T_x signals, respectively. These results, obtained for a diverse range of samples, provide further confirmation that the sensitivity-uncorrected signals (L_x) and the sensitivity (T_x) are capable of measuring much higher doses than can be achieved using the sensitivity-corrected signal (L_x/T_x).

5.3. Recycling ratios

In the standard SAR procedure, after measuring the natural signal (L_n) and its sensitivity (T_n), a series of laboratory doses are given and the induced L_x and T_x signals measured to construct a dose response curve. Regenerative doses are usually chosen so that they bracket the expected natural dose, which is then estimated by projection of the sensitivity-corrected natural signal (L_n/T_n) on to the DRC. One of the laboratory doses is commonly repeated, following the 'double regenerative' procedure introduced by Galbraith et al. (1999). The ratio of the L_x/T_x values obtained for the identical doses should be consistent with unity if no sensitivity change occurred between the two SAR cycles, or if sensitivity changes have been successfully corrected using the T_x signals. This 'recycling ratio' test was, therefore, originally designed to check if T_x can reliably monitor sensitivity changes in L_x. Using conventional SAR procedures, recycling ratios consistent statistically with unity have been reported for the sensitivity-corrected pIRIR and MET-pIRIR signals (L_x/T_x) (Li and Li, 2011; Buylaert et al., 2012), suggesting that the test dose correction works satisfactorily for these procedures in many instances.

For the modified SAR procedure proposed in this study, we determined the ratio between the signal intensities of L_x and T_x obtained from two identical regenerative doses. To avoid confusion with the term 'recycling ratio', which refers to L_x/T_x ratios, we introduce the term 'reproducibility ratio' here to describe the intensity ratios obtained separately for L_x and T_x from two repeat regenerative doses. A reproducibility ratio that is equal or close to unity is an important indicator of negligible sensitivity change in L_x or T_x between SAR cycles, and such ratios would suggest that the 2 hr solar simulator bleach (step 15 in Table 2b) can effectively reset the sensitivity after each SAR cycle. Fig. 7 shows the recycling ratios of L_x/T_x, and the reproducibility ratios of L_x and T_x for 55 aliquots of the Eurasian samples investigated in this study. The mean values of the recycling and reproducibility ratios are 0.98, 1.00 and 1.02 for L_x/T_x, L_x and T_x, respectively, with relative standard deviations of 3%, 3%, and 4%, respectively. These results suggest that the pre-dose dependent sensitivity change can be effectively reset by the solar bleaching step applied between each SAR cycle, thereby providing further support for the reliability of the L_x and T_x DRCs (Fig. 6b and c). We

acknowledge, however, that although we can reproduce (or recycle) the data points used to construct DRCs in the laboratory, this does not guarantee that they accurately recreate the form of DRCs in nature. To prove the latter requires measurement of a large number of samples with firm chronological control to permit a direct comparison of the laboratory and natural DRCs. Further studies are therefore required, using more samples of different ages from various regions, to test the accuracy of the DRCs generated in the laboratory.

5.4. Dose recovery and fading test

A critical assumption of the SAR procedure is that the T_n signal induced by a test dose given after the measurement of the natural signal (L_n) accurately reflects the sensitivity of L_n. The validity of this assumption is usually tested using a dose recovery experiment (following Galbraith et al., 1999), which involves giving a known laboratory dose to bleached aliquots. The given dose is then measured as a surrogate natural dose to test if the SAR procedure can recover the correct (known) dose. A successful dose recovery test cannot guarantee that the D_e estimation will be estimated correctly, but a failed dose recovery test would cast doubt on the accuracy of the D_e estimates obtained using the same experimental conditions.

In this study, a 'delayed dose recovery test'—similar to those used in previous studies (Li and Li, 2011; Li et al., 2013b)—was conducted on samples Sm8, CEP-OSL1 and PIN-OSL2, to test the reliability of the modified SAR procedure and check for anomalous fading of the MET-pIRIR signals. In this test, 3–6 aliquots from each sample were first bleached using the solar simulator for ~4 hr, after which the aliquots of samples Sm8 and CEP-OSL1 were given a laboratory dose of 1100 Gy, and aliquots of PIN-OSL2 were given a dose of 770 Gy. These aliquots were then stored in the dark for 120 days (Sm8 and PIN-OSL2) or 36 days (CEP-OSL1) before the doses were measured using the modified SAR MET-pIRIR procedure shown in Table 2b. The time differences between the delayed measurements of the surrogate 'natural' doses and the prompt measurements of the subsequent

425 regenerative doses amount to ~2.8, 3.4 and 3.3 decades for Sm8, CEP-OSL1 and PIN-OSL2,
426 respectively.

427 The measured to given dose ratios of L_x and T_x for the MET-pIRIR signals from these 3
428 samples are shown in Fig. 8; a similar pattern was observed for the samples. For L_x/T_x, the delayed
429 dose recovery ratio was underestimated by 20–47% for the 50 °C IRSL signal. The extent of
430 underestimation in L_x/T_x is reduced at higher stimulation temperatures and is negligible at 200 °C for
431 CEP-OSL1 and PIN-OSL2 and at 250 °C for Sm8. We interpret these trends as indicating that the
432 MET-pIRIR L_x/T_x signals at elevated temperatures (>200 °C) have negligible fading rates and can
433 recover, with reasonable accuracy, the known dose. A similar pattern was observed for L_x. It appears,
434 however, that a lower extent of underestimation was observed for the T_x at low stimulation
435 temperatures (e.g. 50 and 100 °C) for samples CEP-OSL1 and Sm8. A reliable result from the 50 °C
436 IRSL signal could not be obtained for T_x because the limited change in sensitivity with dose (Fig. 3c).

437 Unlike the results of L_x/T_x and L_x, however, the delayed dose recovery ratios for T_x (shown as
438 triangles in Fig. 8) are statistically consistent with unity at IR stimulation temperatures of 150 °C and
439 above for all 3 samples. As T_x is always measured after the same delay following irradiation and
440 preheating, any anomalous fading in T_x refers to the pre-dose memory of T_x (that is, the number of
441 hole centers) rather than to the charge in the electron traps. Thus, delayed dose recovery ratios of
442 unity for T_x indicate that the hole centres are more stable—that is, they exhibit less fading—than the
443 electrons in the IRSL traps (represented by the L_x and L_x/T_x signals).

444

445 5.5. Age estimation using the new pMET-pIRIR procedure

446 To further test the applicability of the modified SAR procedure for MET-pIRIR signals, we
447 used it to obtain D_e values for all of the samples in Table 1, as well as age estimates for the samples
448 from Les Cottés, Luochuan and Shimao for which the environmental dose rates and independent age

449 controls are also available. The D_e values and ages calculated for the L_x/T_x, L_x and T_x MET-pIRIR
450 signal stimulated at 250 ºC are summarised in Table 1, and the D_e values obtained from the different
451 signals are plotted against IR stimulation temperature in Fig. 9. The latter plots are similar to the Age–
452 Temperature (A–T) plots used in previous MET-pIRIR studies (Li and Li, 2011; 2012).

453 The D_e–Temperature plots (Fig. 9) share a common feature: the D_e values increase with
454 stimulation temperature, and D_e values consistent with the expected values (shown as ± 1σ grey bands
455 for the samples with independent age controls) are often reached at higher temperatures (e.g. >200
456 °C), indicating that a non-fading component has been isolated. Independent ages are not available for
457 samples DHB2-OSL4, CEP-OSL1 or PIN-OSL2, but the D_e values obtained at higher temperatures
458 are statistically consistent with each other and the 'plateau' regions are shown as dashed lines in Fig.
459 9. Except for sample LC-110, the D_e values obtained from the T_x signal are generally higher than or
460 equal to those obtained from L_x and L_x/T_x at stimulation temperatures of less than 200 °C. At 250 °C,
461 however, the D_e values from all 3 signals are statistically consistent with each other.

462 Age plateaux were obtained from the T_x signal stimulated at temperatures of 200 °C and
463 higher, indicating that a stable non-fading component was present in all samples. The only exception
464 appears to be Sm5, which gave D_e underestimates (albeit consistent with the expected values at 2σ)
465 from all 3 signals, although no such underestimation was obtained using the multiple-aliquot pMET-
466 pIRIR procedure (Li et al., 2013b). The results for T_x contrast with those for L_x/T_x, which does not
467 yield a plateau in D_e, even at the highest stimulation temperature (250 °C). Li and Li (2012) observed
468 that a plateau could only be reached at temperatures of 250 °C and higher for samples older than ~130
469 ka. This result confirms the findings of the delayed dose recovery test (Fig. 8): namely, that the
470 sensitivity of the pMET-pIRIR signal (T_x)—the hole centres—is probably more stable than the
471 population of electrons in the IRSL traps (L_x/T_x).

472 As a final check that the extent of anomalous fading is negligible at elevated stimulation
473 temperatures (>200 °C), we compared the ages obtained from the 250 ºC MET-pIRIR signals with the

474 independently known ages of the samples from Luochuan, Shimao and Les Cottés. The ages
475 determined from the L_x/T_x, L_x and T_x signals are plotted against the expected ages in Fig. 10a, b and c,
476 respectively. The L_x/T_x signal at 250 ºC appears to give reliable ages of up to ~350 ka, above which it
477 then slightly underestimates the ages of the oldest sample, Sm8 (Fig. 10a). The D_e values of the three
478 oldest samples (LC-270, Sm6' and Sm8) are more than twice the value of the characteristic saturation
479 dose of the L_x/T_x signal ($2D_0$ ~700–800 Gy) (see Fig. 6a); this is sometimes used as a conservative
480 upper limit for reliable D_e determination (Wintle and Murray, 2006), although there is no statistical
481 impediment to estimate higher D_e values (Galbraith and Roberts, 2012). At IR stimulation
482 temperatures of less than 250 ºC, the L_x/T_x ages are consistently too young for samples older than
483 ~130 ka. A similar pattern is observed for the L_x ages, although the degree of age underestimation is
484 smaller at all elevated temperatures and the ages obtained at 250 ºC are consistent (at 2σ) with the
485 expected ages of all of the samples (Fig. 10b). The latter applies also to the T_x ages, which also show
486 good agreement with the expected ages at IR stimulation temperatures as low as 200 ºC (Fig. 10c).
487 The natural doses of the studied samples are below, or close to, the $2D_0$ values of the L_x and T_x signals
488 (~1500–1600 Gy) (Fig. 6b, c), which may have contributed to the determination of accurate D_e values
489 and ages. We consider, therefore, that the L_x and T_x signals stimulated at 250 ºC produce reliable ages
490 for our samples.

491 **6. Discussion**

492 Based on measurements of single aliquots of K-feldspar, we observed a significant
493 dependence of the sensitivity of pIRIR signals on irradiation and solar bleaching, which supports our
494 recent findings made using multiple aliquots (Li et al., 2013b). We attribute this dose dependence of
495 sensitivity mainly to changes in the probability of radiative recombination during IRSL and pIRIR
496 measurements, resulting from changes in the number of hole centres that have a much higher
497 characteristic saturation dose (D_0 ~700–800 Gy) than the pIRIR electron traps (D_0 ~300–400 Gy)
498 (Fig. 3 and 5). This dose dependence can be reset by exposing the sample to sunlight, as demonstrated

499 by the solar simulator bleaching experiment (Li et al., 2013b), sensitivity change test (section 5.1) and
500 reproducibility ratio test (section 5.3). In contrast, a hot IR bleach at the end of each SAR cycle does
501 not achieve the same effect as a solar simulator bleach and can result in an increase in L_x and T_x over
502 successive SAR cycles (Fig. 2b and 2c). This indicates that the pIRIR signal (L_x) and its sensitivity
503 (T_x) may progressively build up from cycle to cycle due to the less effective bleaching of IR radiation
504 compared to the solar simulator spectrum. Within the same SAR cycle, therefore, the residual signal
505 associated with L_x is likely to be included in the subsequent T_x measurement, because no solar bleach
506 is employed between the L_x and T_x measurements in the same SAR cycle. As the L_x signal is dose
507 dependent (Fig. 3b), the dose dependency in T_x (Fig. 3c) may partly arise from the carry-over of
508 residual charge from the preceding L_x measurement. This will not affect the dating results, however,
509 because L_x and T_x do not build up from one SAR cycle to the next when a solar simulator bleach is
510 applied at the end of each cycle (Fig. 2b and 2c). So, from these lines of evidence and others
511 presented above, we conclude that the sensitivity-uncorrected signal (L_x) and its dose-dependent
512 sensitivity (T_x) are suitable for dating sediments, provided that a solar simulator bleach is included in
513 the SAR procedure (Table 2b). The high saturation levels of these signals allow the IRSL dating range
514 to be extended into the Middle and, possibly, Early Pleistocene.

515 We have shown that the multiple-aliquot pMET-pIRIR method (Table 2a) proposed by Li et
516 al. (2013b) may not be applicable to samples that exhibit large variation in sensitivity among separate
517 grains or aliquots (Fig. 1). To overcome this problem, we have developed a single-aliquot procedure
518 to exploit the dose-dependent pIRIR sensitivity. This modified SAR procedure employs a 2 hr solar
519 simulator bleach at the end of each SAR cycle (Table 2b), instead of the usual high temperature
520 ('hot') IR bleach (e.g. Buylaert et al., 2009; Li and Li, 2011). Our single-aliquot procedure overcomes
521 the problem associated with aliquot-to-aliquot variations in the optical, thermal and pre-dose histories
522 of the constituent grains (section 4), and has allowed us to construct DRCs of L_x and T_x for samples
523 that are not amenable to multiple-aliquot approach; compare, for example, Fig. 1 and 3 for sample
524 CEP-OSL1.

A key feature of the modified SAR method is that the 3 signals (L_x/T_x, L_x and T_x) obtained in the same experimental sequence are each suitable for dating, but with advantages and disadvantages specific to each signal (Table 3). Although the sensitivity-corrected signal (L_x/T_x) has the youngest upper age limit due to its low saturation dose level, it is also less dependent on the measurement conditions (e.g. preheat temperature) than either L_x or T_x (Fig. 2). In contrast, the sensitivity (T_x) has a much higher saturation dose level, but a larger measurement uncertainty compared to L_x/T_x (Fig. 8 and 9), presumably due to the limited range of dose dependency—that is, the intensity of the MET-pIRIR T_x signal at 250 °C increases by only 3–4 times over the dose range 0 to ~3000 Gy (Fig. 3 and 5). On the other hand, T_x does not have residual dose problems associated with un-bleachable signals, which can potentially influence the accuracy of the age obtained for samples that have large residual signal (Li et al., 2013a). The sensitivity-uncorrected signal (L_x) is measured with higher precision than T_x and has a much larger saturation dose than L_x/T_x (Fig. 3 and 5). Given the various advantages and disadvantages of these signals, we recommend that D_e values and ages should be obtained using all 3 of them to provide a cross-check on the dating results.

By studying sediment samples from different regions of Eurasia, we have found that the dose-dependency of the pIRIR signals is a common phenomenon (Fig. 6). Furthermore, there might be a common DRC among different samples of K-feldspar (Fig. 6) that would allow a 'standardized growth curve' (SGC) procedure to be developed for feldspar as was originally proposed for quartz (Roberts and Duller, 2004; Lai, 2006). A SGC procedure would greatly reduce the time required to date older samples, as up to several thousands of Gy are typically delivered to each aliquot in each SAR cycle. Further study on the potential of a SGC approach for feldspar dating is warranted.

A drawback, however, of using a solar simulator bleach step at the end of each SAR cycle is that aliquots must be moved between the OSL/TL reader and the solar simulator, and this may result in the loss of grains from some aliquots. It is important, therefore, to be extremely careful when conducting such experiments. The issue can be solved by using a TL/OSL reader with an attached solar bleaching facility (e.g. Bøtter-Jensen et al., 2003), but this will significantly increase the

measurement time because each aliquot is bleached individually. In contrast, many tens of aliquots can be bleached simultaneously using a separate the solar simulator. For single-grain dating, however, an attached bleaching source would permit the simultaneous illumination of 100 grains, without requiring movement of the discs to a separate solar simulator.

7. Conclusions

We have described and tested a modified SAR procedure for measuring the IRSL signals from K-feldspars. The new pMET-pIRIR procedure utilises the dose-dependent sensitivity of the pIRIR signals measured at elevated temperature (e.g. 250 ºC). A 2 hr solar simulator bleach is used to reset the dose-dependent sensitivity at the end of each regenerative SAR cycle. A key feature of this method is that D_e values can be obtained using either the regenerative signal (L_x) or the test dose signal (T_x), both of which saturate at a higher dose than the sensitivity-corrected signal (L_x/T_x), thereby extending the dating limit beyond that achievable using conventional pIRIR methods. Studies on various sediments from Europe and Asia show that this dose-dependent sensitivity—in effect, a memory of the pre-dose received by sample in nature—is a common phenomenon among K-feldspars, so this new method has the potential to be applied widely to sedimentary deposits worldwide. Based on laboratory dose recovery tests and on comparisons with independent age controls, we conclude that this single-aliquot pMET-pIRIR procedure is capable of measuring natural doses of up to ~1500 Gy, which conservatively permits dating of sediments deposited as early as 400–800 ka ago at environmental dose rates of 2–4 Gy/ka. This opens up the possibility of using K-feldspars to date events in the Late and Middle Pleistocene. The new SAR procedure described here also makes single-grain dating of K-feldspars a practicable option, and thus enables the investigation of sediments that were heterogeneously bleached at the time of deposition or were subjected to disturbance thereafter.

Acknowledgements

This study was supported by a University of Wollongong Vice-Chancellor's Postdoctoral Research Fellowship to Li, and by Australian Research Council grants and fellowships to Roberts (DP0880675) and Jacobs (DP1092843), and by the Research Grant Council of the Hong Kong Special Administrative Region, China, to SHL (7028/08P). We thank Dan Adler and Claudio Tuniz for providing samples PIN-OSL2 and CEP-OSL1, respectively; Yasaman Jafari for assistance with sample preparation; and both anonymous reviewers for their constructive comments.

References

Adamiec, G., Aitken, M.J., 1998. Dose-rate conversion factors: update. Ancient TL 16, 37–50.

Aitken, M.J., 1998. An Introduction to Optical Dating. Oxford University Press, Oxford.

Bøtter-Jensen, L., Bulur, E., Duller, G.A.T., Murray, A.S., 2000. Advances in luminescence instrument systems. Radiation Measurements 32, 523–528.

Bøtter-Jensen, L., Andersen, C.E., Duller, G.A.T., Murray, A.S., 2003. Developments in radiation, stimulation and observation facilities in luminescence measurements. Radiation Measurements 37, 535–541.

Buylaert, J.P., Jain, M., Murray, A.S., Thomsen, K.J., Thiel, C., Sohbati, R., 2012. A robust feldspar luminescence dating method for Middle and Late Pleistocene sediments. Boreas 41, 435–451.

Buylaert, J.P., Murray, A.S., Thomsen, K.J., Jain, M., 2009. Testing the potential of an elevated temperature IRSL signal from K-feldspar. Radiation Measurements 44, 560–565.

Ding, Z.L., Derbyshire, E., Yang, S.L., Yu, Z.W., Xiong, S.F., Liu, T.S., 2002. Stacked 2.6-Ma grain size record from the Chinese loess based on five sections and correlation with the deep-sea delta O-18 record. Paleoceanography 17, 5-1.

Fu, X., Li, B., Li, S.H., 2012. Testing a multi-step post-IR IRSL dating method using polymineral fine grains from Chinese loess. Quaternary Geochronology 10, 8–15.

Galbraith, R.F., Roberts, R.G., Laslett, G.M., Yoshida, H., Olley, J.M., 1999. Optical dating of single and multiple grains of quartz from Jinmium rock shelter, northern Australia: Part I, experimental design and statistical models. Archaeometry 41, 339–364.

Galbraith, R.F., Roberts, R.G., 2012. Statistical aspects of equivalent dose and error calculation and display in OSL dating: an overview and some recommendations. Quaternary Geochronology 11, 1–27.

Guérin, G., 2006. Some aspects of phenomenology and kinetics of high temperature thermoluminescence of plagioclase feldspars. Radiation Measurements 41, 936–941.

Huntley, D.J., Baril, M.R., 1997. The K content of the K-feldspars being measured in optical dating or in thermoluminescence dating. Ancient TL 15, 11–13.

Huntley, D.J., Hancock, R.G.V., 2001. The Rb contents of the K-feldspars being measured in optical dating. Ancient TL 19, 43–46.

Huntley, D.J., Lamothe, M., 2001. Ubiquity of anomalous fading in K-feldspars and the measurement and correction for it in optical dating. Canadian Journal of Earth Sciences 38, 1093–1106.

Huntley, D.J., Lian, O.B., 2006. Some observations on tunnelling of trapped electrons in feldspars and their implications for optical dating. Quaternary Science Reviews 25, 2503–2512.

Jain, M., Singhvi, A.K., 2001. Limits to depletion of blue-green light stimulated luminescence in feldspars: implications for quartz dating. Radiation Measurements 33, 883–892.
Kars, R.H., Wallinga, J., Cohen, K.M., 2008. A new approach towards anomalous fading correction for feldspar IRSL dating — tests on samples in field saturation. Radiation Measurements 43, 786–790.
Lai, Z.P., 2006. Testing the use of an OSL standardised growth curve (SGC) for D_e determination on quartz from the Chinese Loess Plateau. Radiation Measurements 41, 9–16.
Lamothe, M., Auclair, M., 1999. A solution to anomalous fading and age shortfalls in optical dating of feldspar minerals. Earth and Planetary Science Letters 171, 319–323.
Lamothe, M., Auclair, M., Hamzaoui, C., Huot, S., 2003. Towards a prediction of long-term anomalous fading of feldspar IRSL. Radiation Measurements 37, 493–498.
Li, B., Jacobs, Z., Roberts, R.G., Li, S.H., 2013b. Extending the age limit of luminescence dating using the dose-dependent sensitivity of MET-pIRIR signals from K-feldspar. Quaternary Geochronology 17, 55–67.
Li, B., Li, S.H., 2008. Investigations of the dose-dependent anomalous fading rate of feldspar from sediments. Journal of Physics D–Applied Physics 41, 225502.
Li, B., Li, S.H., 2011. Luminescence dating of K-feldspar from sediments: a protocol without anomalous fading correction. Quaternary Geochronology 6, 468–479.
Li, B., Li, S.H., 2012. Luminescence dating of Chinese loess beyond 130 ka using the non-fading signal from K-feldspar. Quaternary Geochronology 10, 24–31.
Li, B., Li, S.H., Duller, G.A.T., Wintle, A.G., 2011. Infrared stimulated luminescence measurements of single grains of K-rich feldspar for isochron dating. Quaternary Geochronology 6, 71–81.
Li, B., Li, S.H., Wintle, A.G., Zhao, H., 2007. Isochron measurements of naturally irradiated K-feldspar grains. Radiation Measurements 42, 1315–1327.
Li, B., Li, S.H., Wintle, A.G., Zhao, H., 2008. Isochron dating of sediments using luminescence of K-feldspar grains. Journal of Geophysical Research–Earth Surface 113, F02026.
Li, B., Roberts, R.G., Jacobs, Z., 2013a. On the dose dependency of the bleachable and non-bleachable components of IRSL from K-feldspar: improved procedures for luminescence dating of Quaternary sediments. Quaternary Geochronology 17, 1–13.
Murray, A.S., Roberts, R.G., 1998. Measurement of the equivalent dose in quartz using a regenerative-dose single-aliquot protocol. Radiation Measurements 29, 503–515.
Murray, A.S., Wintle, A.G., 2000. Luminescence dating of quartz using an improved single-aliquot regenerative-dose protocol. Radiation Measurements 32, 57–73.
Roberts, H.M., Duller, G.A.T., 2004. Standardised growth curves for optical dating of sediment using multiple-grain aliquots. Radiation Measurements 38, 241–252.
Sanderson, D.C.W., Clark, R.J., 1994. Pulsed photostimulated luminescence of alkali feldspars. Radiation Measurements 23, 633–639.
Spooner, N.A., 1994. The anomalous fading of infrared-stimulated luminescence from feldspars. Radiation Measurements 23, 625–632.
Sun, J.M., Ding, Z.L., Liu, T.S., Rokosh, D., Rutter, N., 1999. 580,000-year environmental reconstruction from aeolian deposits at the Mu Us Desert margin, China. Quaternary Science Reviews 18, 1351–1364.
Talamo, S., Soressi, M., Roussel, M., Richards, M., Hublin, J., 2012. A radiocarbon chronology for the complete Middle to Upper Palaeolithic transitional sequence of Les Cottés (France). Journal of Archaeological Science 39, 175–183.
Thiel, C., Buylaert, J.P., Murray, A., Terhorst, B., Hofer, I., Tsukamoto, S., Frechen, M., 2011. Luminescence dating of the Stratzing loess profile (Austria) — testing the potential of an elevated temperature post-IR IRSL protocol. Quaternary International 234, 23–31.
Thomsen, K.J., Murray, A.S., Jain, M., Botter-Jensen, L., 2008. Laboratory fading rates of various luminescence signals from feldspar-rich sediment extracts. Radiation Measurements 43, 1474–1486.

667 Tsukamoto, S., Denby, P.M., Murray, A.S., Bøtter-Jensen, L., 2006. Time-resolved luminescence
668 from feldspars: new insight into fading. Radiation Measurements 41, 790–795.
669 Valladas, G., Valladas, H., 1979. High temperature thermoluminescence. Proceedings of the 18th
670 International Symposium on Archaeometry and Archaeological Prospection, Bonn, pp. 506–
671 510.
672 Wintle, A.G., 1973. Anomalous fading of thermoluminescence in mineral samples. Nature 245, 143–
673 144.
674 Wintle, A.G., Murray, A.S., 2006. A review of quartz optically stimulated luminescence
675 characteristics and their relevance in single-aliquot regeneration dating protocols. Radiation
676 Measurements 41, 369–391.
677 Zhao, H., Li, S.H., 2002. Luminescence isochron dating: a new approach using different grain sizes.
678 Radiation Protection Dosimetry 101, 333–338.
679 Zhao, H., Li, S.H., 2005. Internal dose rate to K-feldspar grains from radioactive elements other than
680 potassium. Radiation Measurements 40, 84–93.
681

Figure captions

Figure 1: Multiple-aliquot results of the normalised sensitivity (T1/T2) of the 250 °C MET-pIRIR signals obtained for sample CEP-OSL1 using the MAR procedure proposed by Li et al. (2013b) (Table 2a). Each data point represents the result for a single aliquot.

Figure 2: Plots of L_x/T_x (a), L_x (b) and T_x (c) MET-pIRIR (250 °C) normalised signal intensities obtained from repeat SAR regenerative dose cycles using different preheat temperatures. Values are normalised to those measured in the first cycle. Measurements were made using the procedure in Table 2b and for preheat temperatures of 360 °C (diamonds), 340 °C (squares), 320 °C (triangles) and 300 °C (crosses) for 60 s. Also shown (as open circles) are the corresponding data obtained using the standard MET-pIRIR procedure of Li et al. (2011), which employs a hot IR bleach for 100 s at 300 °C (instead of a 2 hr solar bleach) at the end of each SAR cycle, and a preheat of 300 °C for 60 s. (d) Sensitivity (T_x) of the MET-pIRIR 250 °C signal for samples Sm1, Sm5 and Sm8 plotted against their natural doses (37 ± 4, 508 ± 41 and 1593 ± 114 Gy, respectively) following a 2 hr solar simulator bleach and normalised to unity at 37 Gy. Each data point represents the average results of three aliquots, and the error bars represent 1σ standard deviation.

Figure 3: Representative DRCs for the L_x, T_x and sensitivity-corrected (L_x/T_x) MET-pIRIR signals measured at different stimulation temperatures for a single aliquot of sample CEP-OSL1. (a) DRCs for L_x/T_x and (b) DRCs for L_x, normalised to unity at 550 Gy; (c) DRCs for T_x, normalised to unity at 0 Gy. The natural data points are also shown on the y-axes. All the DRCs in (a), (b) and (c) were fitted using a single saturating exponential function (solid lines). The characteristic saturation dose (D_0) value for each curve is shown on the right-hand side.

Figure 4: (a) The relationship between the intensities of the L_x and T_x signals shown in Fig. 3b and 3c for sample CEP-OSL1. (b) Same as (a) but with all values normalised to a T_x value of unity at zero dose. The dashed lines are the least-squares regression fits. The data obtained from the regenerative doses are shown by closed symbols, while the natural doses are shown by open symbols.

Figure 5: DRCs for the L_x, T_x and sensitivity-corrected (L_x/T_x) MET-pIRIR signals measured at 250 °C for sample CEP-OSL1 using the conventional MET-pIRIR procedure with a hot IR bleach (for 100 s at 320 °C) at the end of each SAR cycle. (a) DRCs for L_x/T_x and (b) DRCs for L_x; (c) DRCs for T_x. All DRCs were normalised to a value of unity at 770 Gy. The natural data points were also shown on the y-axis. The DRCs in (a) and (b) were fitted using a single saturating exponential function (solid lines). The DRC of T_x (c) was not fitted due to the large scatters.

Figure 6: Dose response data for the 250 °C MET-pIRIR signals obtained from different samples from different regions of Eurasia (see Table 1 for details): The L_x/T_x, L_x, and T_x data are shown in (a), (b) and (c), respectively, and have been normalised to a value unity at a dose of 770 Gy for comparison. Each data point is the average results of 4–8 aliquots, and the associated standard errors are smaller than the size of the symbols. The dotted lines in each figure are the DRCs fitted to the data for all samples using a single saturating exponential function, and the natural signals are also plotted on the y-axes.

Figure 7: Histogram of recycling ratios (L_x/T_x) and reproducibility ratios (L_x and T_x) for the 250 °C MET-pIRIR signals obtained from 55 single aliquots of the different study samples. The ratios were estimated from the signals measured for duplicate regenerative doses and have typical standard errors of 2-4%. The histogram bin widths are 0.02 and the two vertical dashed lines delimit ratios of 0.95–1.05.

Figure 8: Measured to given dose ratios for the L_x/T_x, L_x and T_x MET-pIRIR signals, plotted against IR stimulation temperature, for samples (a) CEP-OSL1, (b) PIN-OSL2 and (c) Sm8. Each data point represents the mean value (and standard error) for 3–6 separate aliquots.

Figure 9: The MET-pIRIR D_e values for all study samples obtained from the L_x/T_x, L_x and T_x signals, plotted against IR stimulation temperature. For the 7 samples with independent age control, the horizontal grey bands correspond to the expected D_e values (and 1σ uncertainties), calculated from the environmental dose rates and expected ages (see Table 1). For the other 3 samples (for which independent ages are not available), the D_e plateaux at high temperatures (>200 °C) are shown as horizontal dashed lines. For sample LC10-16, the plotted D_e values for the L_x/T_x and L_x signals have been corrected for the residual doses measured after

bleaching using a solar simulator. For sample CEP-OSL1, the L_x/T_x signal was saturated at the stimulation temperature of 250 °C, so reliable estimates of D_e could not be made.

Figure 10: Ages obtained from the pMET-pIRIR L_x/T_x (a), L_x (b) and T_x (c) signals compared against independently known ages for the samples from Luochuan, Shimao and Les Cottés. A reliable result could not be obtained for the T_x signal measured at 50 °C, owing to the limited change in sensitivity with dose (Fig. 3c).

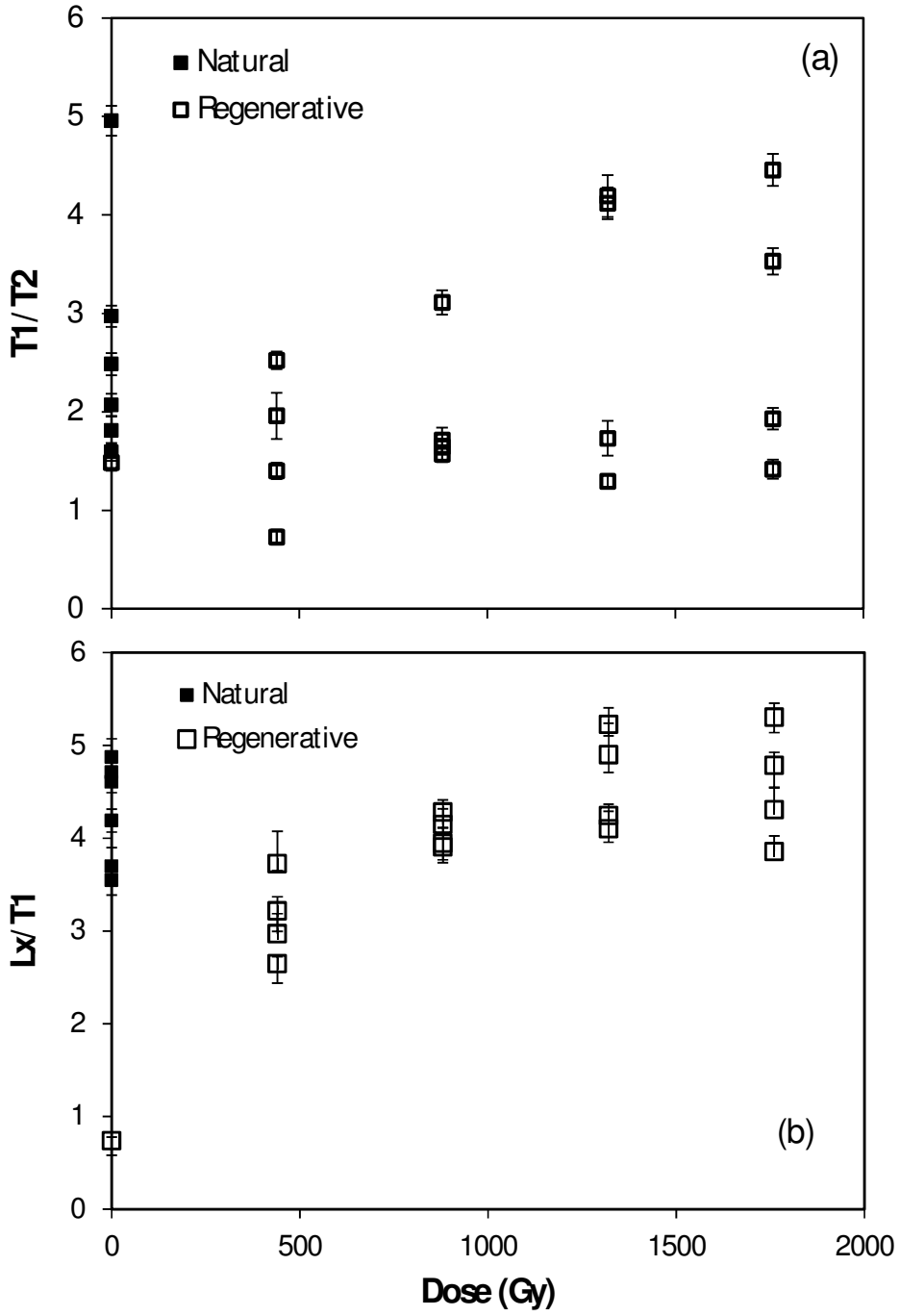
Natural
Regenerative
(a)
T1/T2
Natural
Regenerative
(b)
Lx/T1
Dose (Gy)
0
500
1000
1500
2000

Figure 1

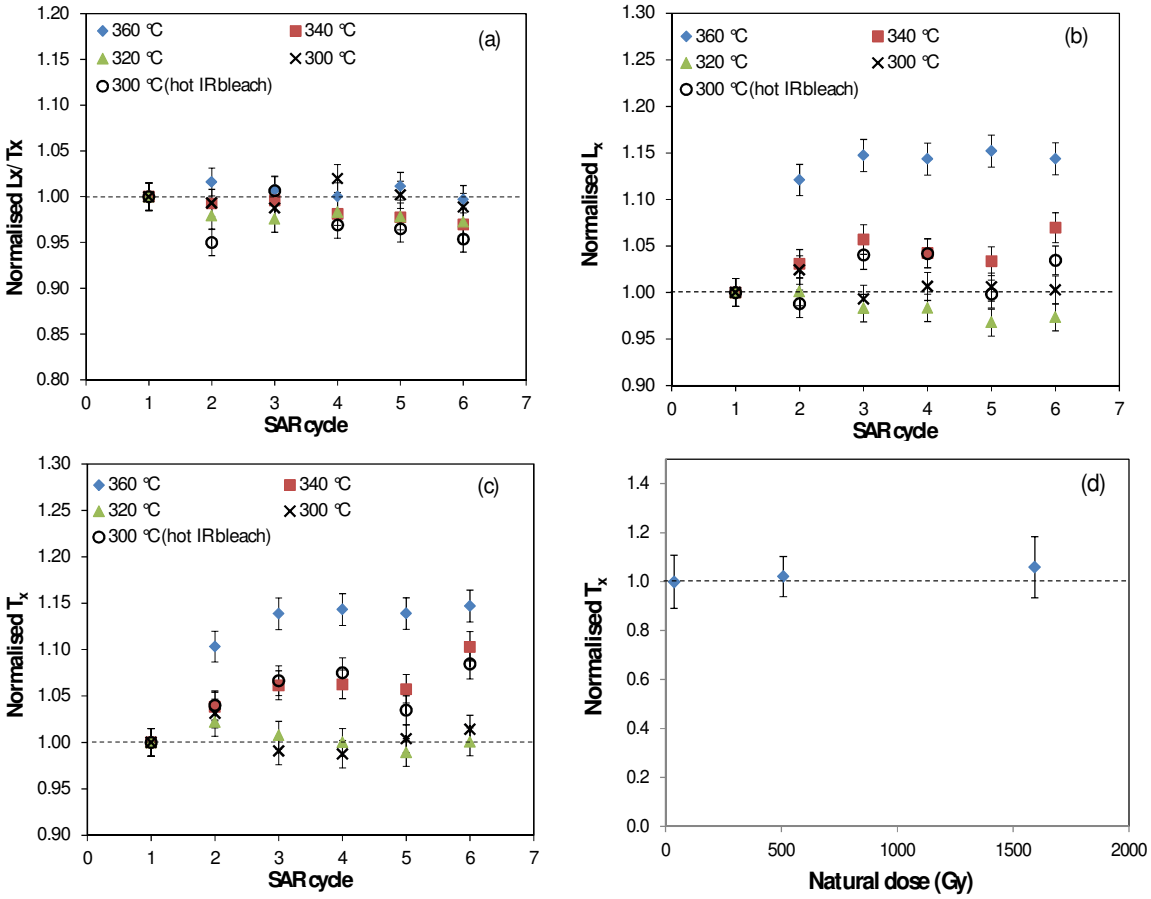
360 ℃
340 ℃
320 ℃
300 ℃
300 ℃(hot IRbleach)
(a)
Normalised Lx/Tx
SAR cycle
(b)
Normalised Lx
(c)
Normalised Tx
(d)
Natural dose (Gy)

Figure 2

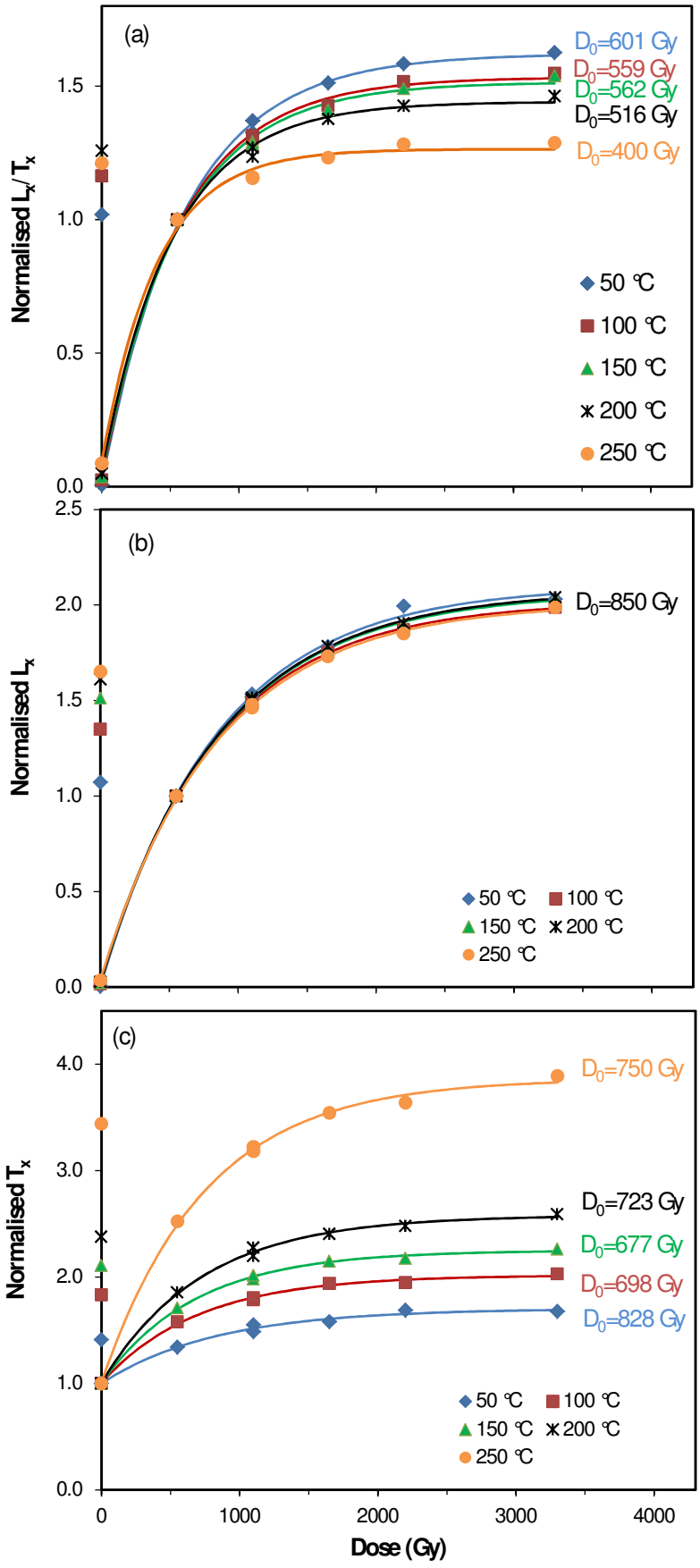
(a)
Normalised L_x/T_x
D_0=601 Gy
D_0=559 Gy
D_0=562 Gy
D_0=516 Gy
D_0=400 Gy
50 ℃
100 ℃
150 ℃
200 ℃
250 ℃
(b)
Normalised L_x
D_0=850 Gy
50 ℃
100 ℃
150 ℃
200 ℃
250 ℃
(c)
Normalised T_x
D_0=750 Gy
D_0=723 Gy
D_0=677 Gy
D_0=698 Gy
D_0=828 Gy
50 ℃
100 ℃
150 ℃
200 ℃
250 ℃
Dose (Gy)

Figure 3

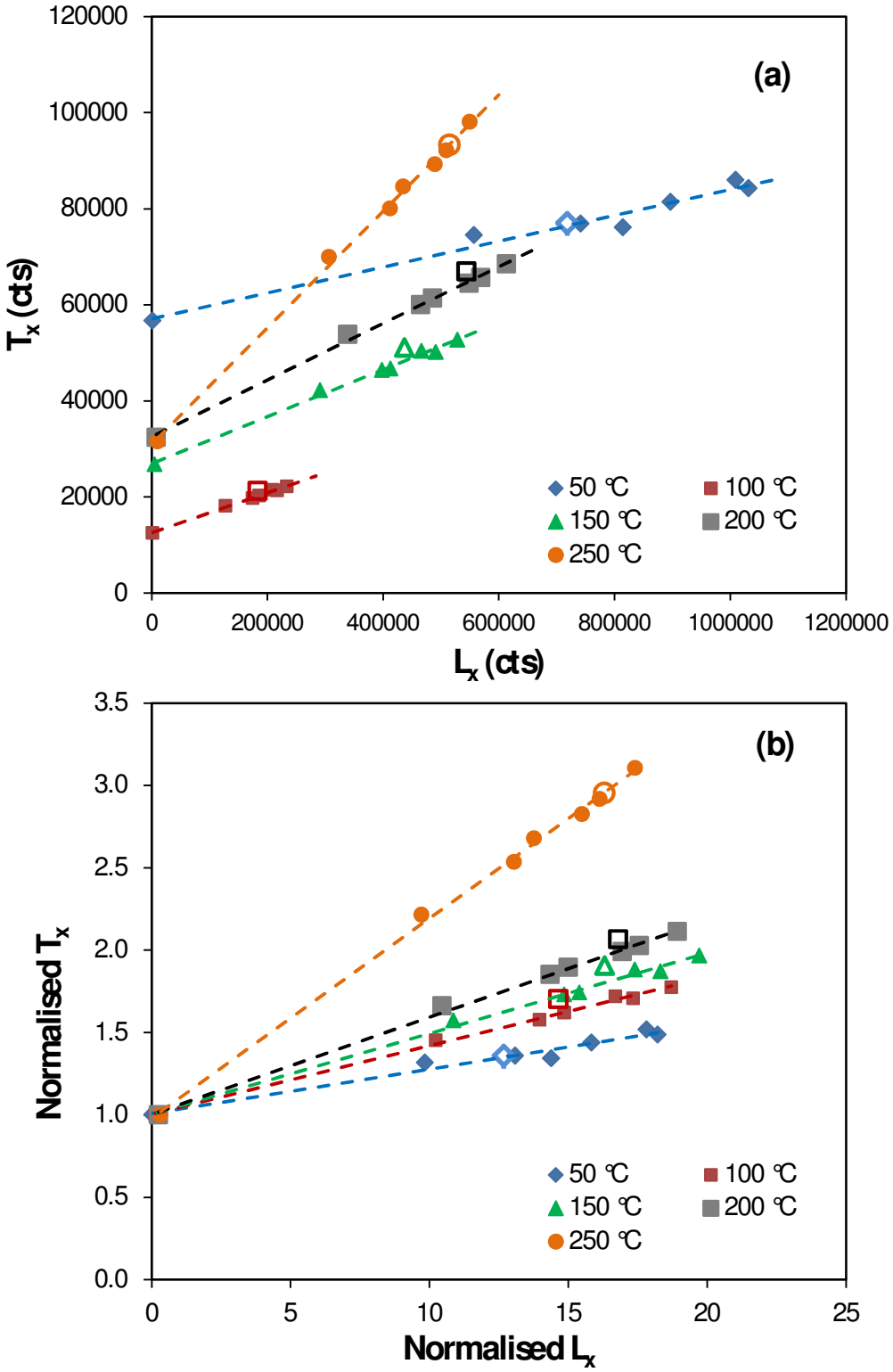
(a)
T_x (cts)
L_x (cts)
120000
100000
80000
60000
40000
20000
0
0
200000
400000
600000
800000
1000000
1200000
50 ℃
100 ℃
150 ℃
200 ℃
250 ℃
(b)
Normalised T_x
Normalised L_x
3.5
3.0
2.5
2.0
1.5
1.0
0.5
0.0
0
5
10
15
20
25
50 ℃
100 ℃
150 ℃
200 ℃
250 ℃

Figure 4

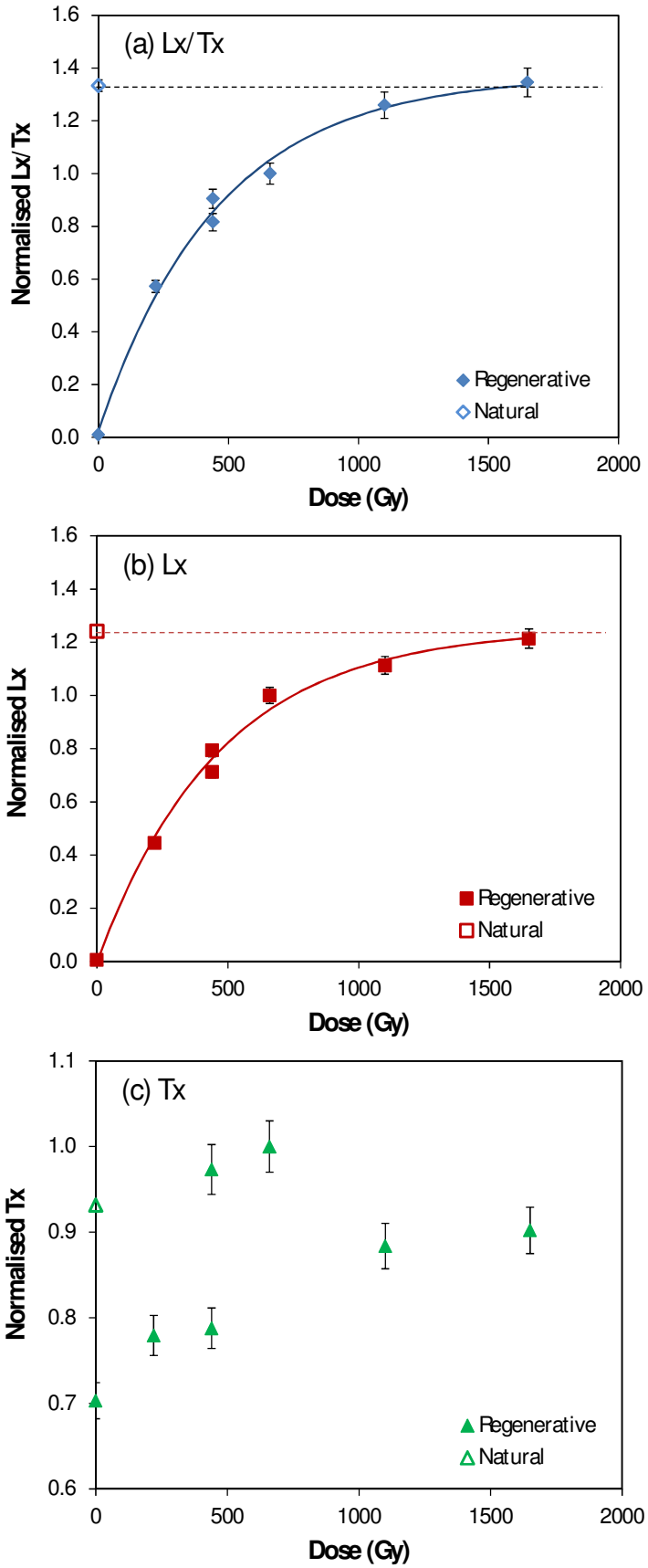
(a) Lx/Tx
Normalised Lx/Tx
Dose (Gy)
Regenerative
Natural
(b) Lx
Normalised Lx
Dose (Gy)
Regenerative
Natural
(c) Tx
Normalised Tx
Dose (Gy)
Regenerative
Natural

Figure 5

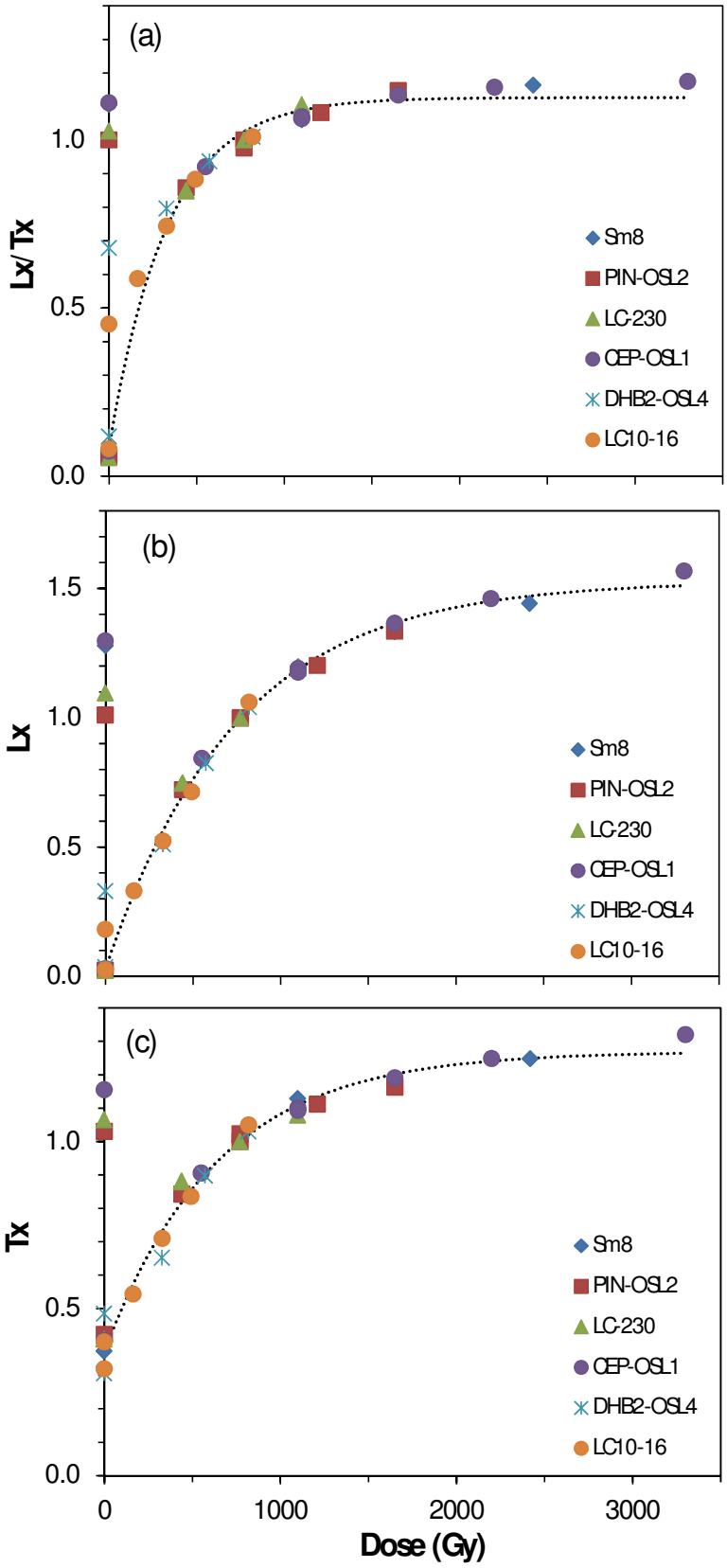
(a)
Lx/Tx
1.0
0.5
0.0
Sm8
PIN-OSL2
LC-230
CEP-OSL1
DHB2-OSL4
LC10-16
(b)
Lx
1.5
1.0
0.5
0.0
Sm8
PIN-OSL2
LC-230
CEP-OSL1
DHB2-OSL4
LC10-16
(c)
Tx
1.0
0.5
0.0
Sm8
PIN-OSL2
LC-230
CEP-OSL1
DHB2-OSL4
LC10-16
0
1000
2000
3000
Dose (Gy)

Figure 6

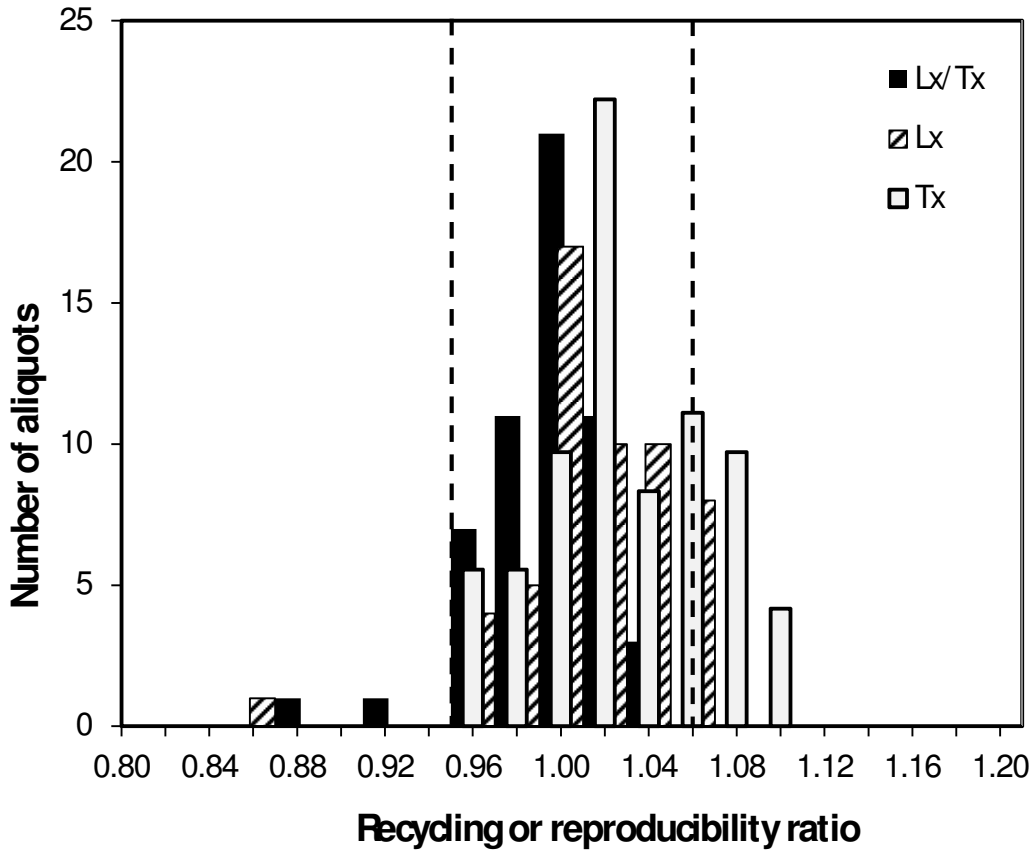
25
20
15
10
5
0
Number of aliquots
0.80
0.84
0.88
0.92
0.96
1.00
1.04
1.08
1.12
1.16
1.20
Recycling or reproducibility ratio
Lx/Tx
Lx
Tx

Figure 7

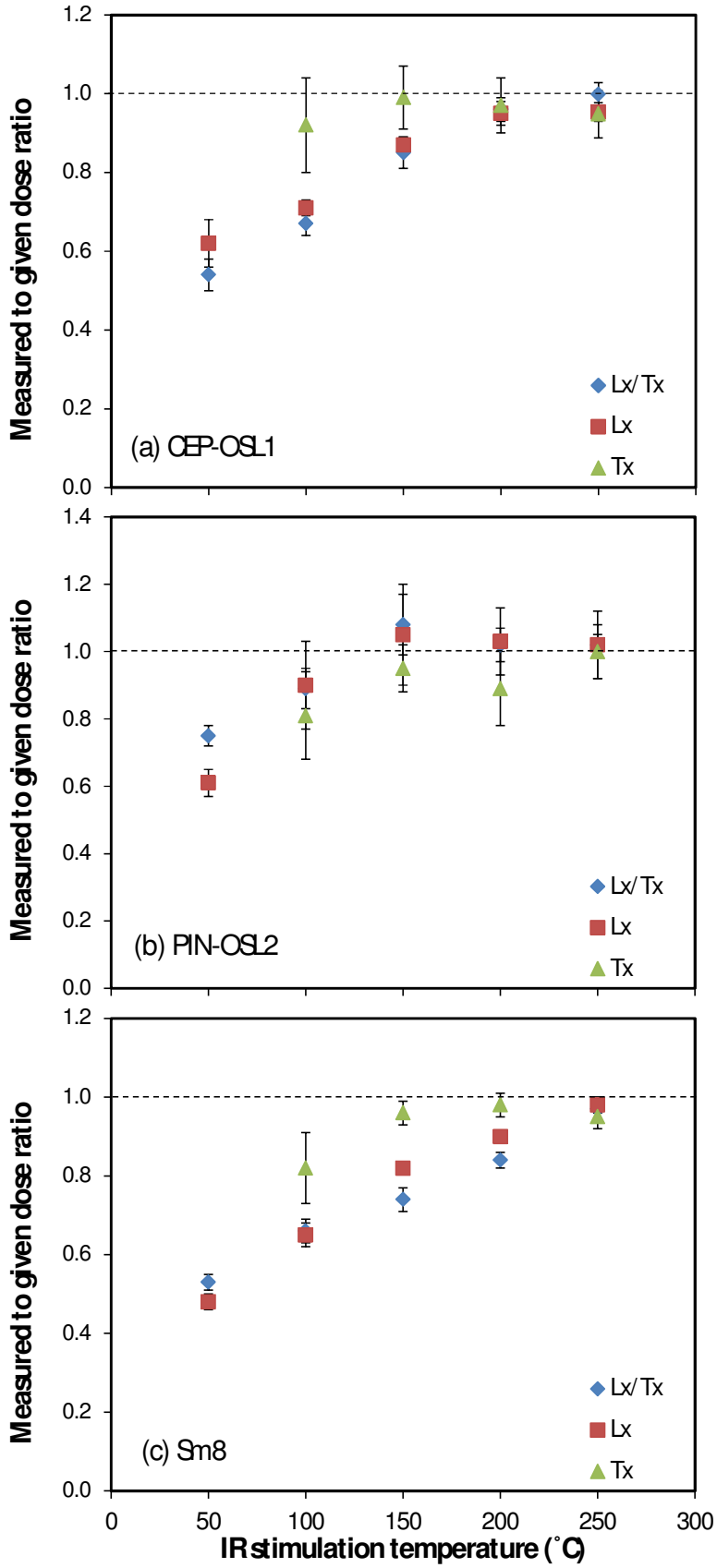
Measured to given dose ratio
1.2
1.0
0.8
0.6
0.4
0.2
0.0
(a) CEP-OSL1
Lx/Tx
Lx
Tx
1.4
1.2
1.0
0.8
0.6
0.4
0.2
0.0
(b) PIN-OSL2
Lx/Tx
Lx
Tx
1.2
1.0
0.8
0.6
0.4
0.2
0.0
(c) Sm8
Lx/Tx
Lx
Tx
0
50
100
150
200
250
300
IR stimulation temperature (˚C)

Figure 8

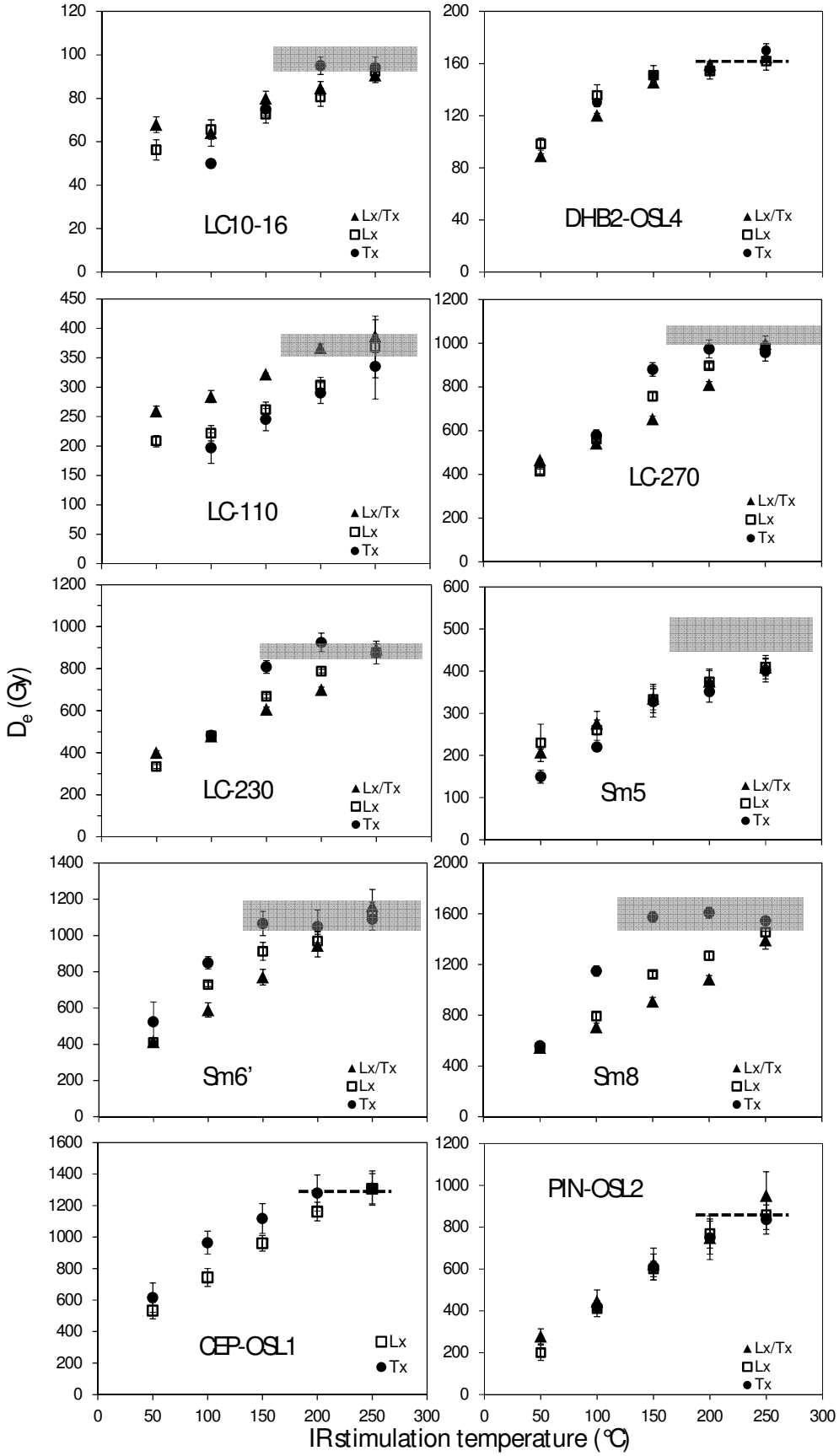
LC10-16
DHB2-OSL4
LC-110
LC-270
LC-230
Sm5
Sm6'
Sm8
CEP-OSL1
PIN-OSL2
▲Lx/Tx
□Lx
●Tx
De (Gy)
IR stimulation temperature (°C)

Figure 9

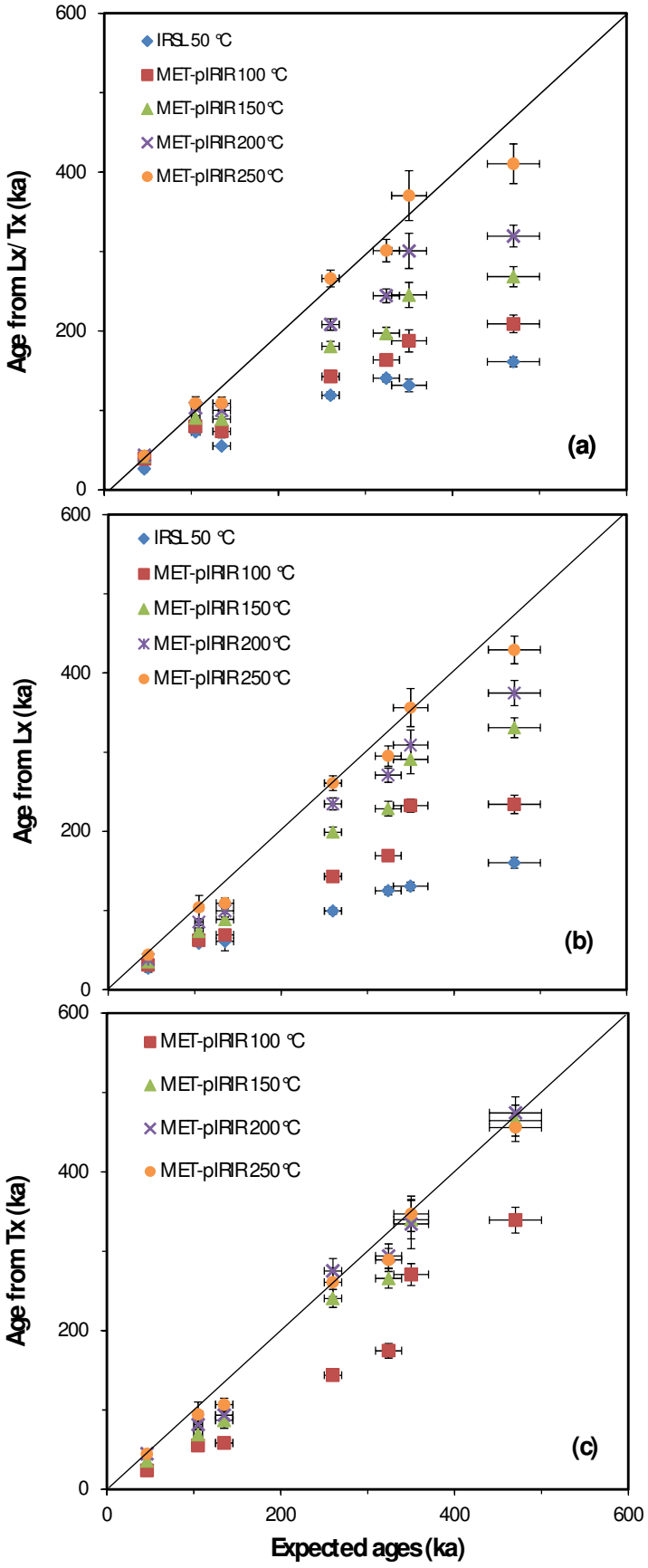
IRSL 50 °C
MET-pIRIR100 °C
MET-pIRIR150°C
MET-pIRIR200°C
MET-pIRIR250°C
Age from Lx/ Tx (ka)
(a)
Age from Lx (ka)
(b)
Age from Tx (ka)
(c)
0
200
400
600
Expected ages (ka)

Figure 10

Table 1: Summary of measured grain size, dose rate, expected age, and expected equivalent dose (D_e) for each study sample, together with the D_e and age measured using the 250 ºC MET-pIRIR signal.

Sample	Location	Grain size	Expected age [a]	Dose rate [b]	Expected D_e [a]	D_e (MET-pIRIR 250ºC) (Gy)			Age (MET-pIRIR 250ºC) (ka)		
		(µm)	(ka)	(Gy/ka)	(Gy)	L_x/T_x	L_x	T_x	L_x/T_x	L_x	T_x
LC10-16 [c]	France	90–125	47.9 ± 3.3	2.1 ± 0.1	101 ± 5	112 ± 4	114 ± 5	94 ± 9	42 ± 3	43 ± 4	45 ± 5
LC-110	CLP, China	63–90	105 ± 5	3.6 ± 0.1	372 ± 18	386 ± 28	368 ± 52	335 ± 55	109 ± 9	104 ± 15	94 ± 16
LC-230	CLP, China	63–90	260 ± 10	3.4 ± 0.1	874 ± 34	894 ± 24	877 ± 18	877 ± 55	266 ± 11	261 ± 9	261 ± 18
LC-270	CLP, China	63–90	324 ± 15	3.3 ± 0.1	1072 ± 50	997 ± 36	977 ± 31	957 ± 38	301 ± 15	295 ± 13	289 ± 14
Sm5	MUD, China	180–212	135 ± 10	3.8 ± 0.2	508 ± 41	409 ± 28	410 ± 27	402 ± 27	109 ± 8	109 ± 7	107 ± 8
Sm6'	MUD, China	90–125	350 ± 20	3.1 ± 0.1	1099 ± 72	1163 ± 91	1118 ± 67	1090 ± 61	370 ± 31	356 ± 24	347 ± 22
Sm8	MUD, China	150–180	470 ± 10	3.4 ± 0.1	1593 ± 114	1392 ± 74	1455 ± 36	1545 ± 32	410 ± 25	429 ± 17	456 ± 17
DHB2-OSL4	India	125–180	LP	-	-	183 ± 6	180 ± 21	170 ±15	-	-	-
CEP-OSL1	Italy	125–180	MP	-	-	-	1307 ± 97	1311 ± 109	-	-	-
PIN-OSL2	Georgia	90–180	MP	-	-	951 ± 114	860 ± 71	837 ± 70	-	-	-

Note:

[a] For the samples from Luochuan and Shimao sections, the expected ages are based on stratigraphic comparisons among different sites in the Loess Plateau and on correlations of the grain size and magnetic susceptibility curves to the orbitally tuned Baoji section (Ding et al., 1994); see Sun et al. (1999) for the details of correlation. The expected ages, together with the dose rates, were used to estimate the expected D_e. The expected age of sample LC10-16 is based on the quartz OSL age, which is consistent with the radiocarbon ages of 42.4–43.8 cal. ka BP obtained from bones recovered from the overlying and underlying archaeological layers (Talamo et al., 2012). Based on their archaeological and geological contexts, sample DHB2-OSL4 is expected to be Late Pleistocene (LP) in age and samples PIN-OSL2 and CEP-OSL1 are expected to be of Middle Pleistocene (MP) age.

[b] The dose rates were obtained from measurements of current environmental radioactivity, together with the dose rate conversion factors of Adamiec and Aitken (1998). For calculation of the internal dose rate, the concentrations of ^{40}K and ^{87}Rb are assumed to be 13 ± 1% and 400 ± 100 µg/g, respectively (Huntley and Baril, 1997; Huntley and Hancock, 2001; Zhao and Li, 2005; Li et al., 2007).

[c] For sample LC10-16, a large residual dose of 25 ± 2 Gy in L_x/T_x was obtained for the MET-pIRIR 250 °C after bleaching for 4 hr using a solar simulator, so the age of L_x/T_x has been corrected for this residual dose. The same residual dose was also used to calculate the D_e and age using the L_x signal. We note that there is no residual dose associated with the T_x signal. The residual doses of the Luochuan and Shimao samples are of the order of a few Gy (Li and Li, 2011; Fu et al., 2012); no residual dose correction was applied to these samples, because they are relatively old and the residual signals are negligible compared to their natural signals.

Table 2: (a) Multiple-aliquot regenerative-dose (MAR) and (b) single-aliquot regenerative-dose (SAR) pMET-pIRIR procedures for multiple elevated temperature post-IR IRSL measurements.

(a) MAR procedure (Li et al., 2013b)		
Step	Treatment	Observed
1	Give regenerative dose, D_i [a]	
2	Preheat at 300 °C for 60 s	
3	[b] IRSL measurement at 50 °C for 100 s	$L_{x(50°C)}$
4	[b] IRSL measurement at 100 °C for 100 s	$L_{x(100°C)}$
5	[b] IRSL measurement at 150 °C for 100 s	$L_{x(150°C)}$
6	[b] IRSL measurement at 200 °C for 100 s	$L_{x(200°C)}$
7	[b] IRSL measurement at 250 °C for 100 s	$L_{x(250°C)}$
8	Give test dose, D_t	
9	Preheat at 300 °C for 60 s	
10	[b] IRSL measurement at 50 °C for 100 s	$T1_{(50°C)}$
11	[b] IRSL measurement at 100 °C for 100 s	$T1_{(100°C)}$
12	[b] IRSL measurement at 150 °C for 100 s	$T1_{(150°C)}$
13	[b] IRSL measurement at 200 °C for 100 s	$T1_{(200°C)}$
14	[b] IRSL measurement at 250 °C for 100 s	$T1_{(250°C)}$
15	Cut-heat to 600 °C	
16	Give test dose, D_t	
17	Preheat at 300 °C for 60 s	
18	[b] IRSL measurement at 50 °C for 100 s	$T2_{(50°C)}$
19	[b] IRSL measurement at 100 °C for 100 s	$T2_{(100°C)}$
20	[b] IRSL measurement at 150 °C for 100 s	$T2_{(150°C)}$
21	[b] IRSL measurement at 200 °C for 100 s	$T2_{(200°C)}$
22	[b] IRSL measurement at 250 °C for 100 s	$T2_{(250°C)}$

(b) SAR procedure		
Step	Treatment	Observed
1	Give regenerative dose, D_i [a]	
2	Preheat at 300 °C for 60 s	
3	[b] IRSL measurement at 50 °C for 100 s	$L_{x(50°C)}$
4	[b] IRSL measurement at 100 °C for 100 s	$L_{x(100°C)}$
5	[b] IRSL measurement at 150 °C for 100 s	$L_{x(150°C)}$
6	[b] IRSL measurement at 200 °C for 100 s	$L_{x(200°C)}$
7	[b] IRSL measurement at 250 °C for 100 s	$L_{x(250°C)}$
8	Give test dose, D_t	
9	Preheat at 300 °C for 60 s	
10	[b] IRSL measurement at 50 °C for 100 s	$T1_{(50°C)}$
11	[b] IRSL measurement at 100 °C for 100 s	$T1_{(100°C)}$
12	[b] IRSL measurement at 150 °C for 100 s	$T1_{(150°C)}$
13	[b] IRSL measurement at 200 °C for 100 s	$T1_{(200°C)}$
14	[b] IRSL measurement at 250 °C for 100 s	$T1_{(250°C)}$
15	**Solar simulator bleach for 2 hr**	
16	Return to step 1	

[a] For the 'natural' samples, $D_i = 0$ Gy. The entire sequence is repeated for several regenerative doses, including a zero dose and a repeat dose.

Table 3: Summary of the advantages and disadvantages of L_x/T_x, L_x and T_x for dating.

Signal	Advantages	Disadvantages
L_x/T_x	• Independent of preheat temperature (Fig. 2a)	• Low saturation dose level (Fig. 3a) • Residual dose problem
L_x	• High saturation dose level (Fig. 3b)	• Dependent on preheat temperature (Fig. 2b) • Residual dose problem
T_x	• High saturation dose level (Fig. 3c) • No residual dose problem	• Dependent on preheat temperature (Fig. 2c) • Limited range of dose dependency